

AD-A201 211

DTIC FILE COPY

AFGL-TR-88-0147

**Transient Pulse Monitor**

Jeffrey S. Thayer  
Joseph E. Nanevicz  
David R. Dana

SRI International  
Electromagnetic Sciences Laboratory  
333 Ravenswood Avenue  
Menlo Park, CA 94025

20 May 1988

Scientific Report No. 1

Approved for public release; distribution unlimited

DTIC  
ELECTE  
NOV 03 1988  
S D  
04 H

AIR FORCE GEOPHYSICS LABORATORY  
AIR FORCE SYSTEMS COMMAND  
UNITED STATES AIR FORCE  
HANSCOM AIR FORCE BASE, MASSACHUSETTS 01731-5000

88 11 3 05 6

"This technical report has been reviewed and is approved for publication."

Stephen A. Friske  
STEPHEN A. FRISKE, Capt, USAF  
Contract Manager

Donald A. Gaudet  
for JOHN A. GAUDET, Lt Col, USAF  
Space Systems Technology Branch Chief

FOR THE COMMANDER

Rita C. Sagalyn  
RITA C. SAGALYN  
Division Director

This report has been reviewed by the ESD Public Affairs Office (PA) and is releasable to the National Technical Information Service (NTIS).

Qualified requestors may obtain additional copies from the Defense Technical Information Center. All others should apply to the National Technical Information Service.

If your address has changed, or if you wish to be removed from the mailing list, or if the addressee is no longer employed by your organization, please notify AFGL/DA, Hanscom AFB, MA 01731. This will assist us in maintaining a current mailing list.

Do not return copies of this report unless contractual obligations or notices on a specific document require that it be returned.

UNCLASSIFIED

## SECURITY CLASSIFICATION OF THIS PAGE

## REPORT DOCUMENTATION PAGE

1a. REPORT SECURITY CLASSIFICATION <b>UNCLASSIFIED</b>			1b. RESTRICTIVE MARKINGS	
2a. SECURITY CLASSIFICATION AUTHORITY <b>N/A</b>			3. DISTRIBUTION/AVAILABILITY OF REPORT Approved for public release; distribution unlimited.	
2b. DECLASSIFICATION/DOWNGRADING SCHEDULE <b>N/A</b>				
4. PERFORMING ORGANIZATION REPORT NUMBER(S)			5. MONITORING ORGANIZATION REPORT NUMBER(S) <b>AFGL-TR-88-0147</b>	
6a. NAME OF PERFORMING ORGANIZATION <b>SRI International</b>		6b. OFFICE SYMBOL (if applicable) <b>03652</b>	7a. NAME OF MONITORING ORGANIZATION <b>Air Force Geophysics Laboratory</b>	
6c. ADDRESS (City, State, and ZIP Code) <b>333 Ravenswood Avenue Menlo Park, CA 94025</b>			7b. ADDRESS (City, State, and ZIP Code) <b>Hanscom AFB Massachusetts 01731-5000</b>	
8a. NAME OF FUNDING/SPONSORING ORGANIZATION <b>Air Force Geophysics Laboratory</b>		8b. OFFICE SYMBOL (if applicable) <b>AFGL/PHE</b>	9. PROCUREMENT INSTRUMENT IDENTIFICATION NUMBER <b>F19628-86-C-0231</b>	
8c. ADDRESS (City, State, and ZIP Code) <b>Hanscom AFB, MA 01731-5000</b>			10. SOURCE OF FUNDING NUMBERS	
			PROGRAM ELEMENT NO. <b>63410F</b>	PROJECT NO. <b>2822</b>
			TASK NO. <b>01</b>	WORK UNIT ACCESSION <b>AH</b>
11. TITLE (Include Security Classification) <b>Transient Pulse Monitor</b>				
12. PERSONAL AUTHOR(S) <b>Thayer, J. S.; Nanevicz, J. E.; and Dana, D. R.</b>				
13a. TYPE OF REPORT <b>Scientific Report #1</b>		13b. TIME COVERED <b>FROM 86/9/30 TO 87/9/30</b>	14. DATE OF REPORT (Year, Month, Day) <b>1988 May 20</b>	15. PAGE COUNT <b>70</b>
16. SUPPLEMENTARY NOTATION				
17. COSATI CODES			18. SUBJECT TERMS (Continue on reverse if necessary and identify by block number)	
FIELD	GROUP	SUB-GROUP		
<b>22</b>	<b>02</b>		<b>Spacecraft, Charging, Discharge, Transient, Environment</b>	
19. ABSTRACT (Continue on reverse if necessary and identify by block number)				
<p>SRI International is developing a transient pulse monitor to measure the characteristics of electrostatic discharges on spacecraft. This report describes the design at the critical design review stage (September 1987).</p>				
20. DISTRIBUTION/AVAILABILITY OF ABSTRACT <input type="checkbox"/> UNCLASSIFIED/UNLIMITED <input checked="" type="checkbox"/> SAME AS RPT. <input type="checkbox"/> DTIC USERS			21. ABSTRACT SECURITY CLASSIFICATION <b>UNCLASSIFIED</b>	
22a. NAME OF RESPONSIBLE INDIVIDUAL <b>Stephen A. Friske, Capt., USAF</b>			22b. TELEPHONE (Include Area Code) <b>(617) 377-3992</b>	22c. OFFICE SYMBOL <b>AFGL/PHE</b>

## CONTENTS

LIST OF ILLUSTRATIONS.....	v
LIST OF TABLES.....	vii
GLOSSARY.....	ix
1.0 INTRODUCTION.....	1
1.1 The IMPS Program.....	1
1.2 Role of the Transient Pulse Monitor.....	2
2.0 BACKGROUND.....	5
2.1 Experimental Studies.....	5
2.1.1 Orbital Particle Environment.....	6
2.1.2 Particle Interactions with Satellite Materials: Charging.....	6
2.1.3 Discharges and Their Effects on Systems.....	6
2.1.4 Fixes.....	7
2.2 Current Understanding of the Technical Areas.....	7
2.2.1 Orbital Particle Environment.....	7
2.2.2 Particle Interactions with Satellite Materials: "Surface" Charging.....	7
2.2.3 Discharges and Their Effects on Systems.....	9
2.2.4 Fixes.....	11
2.2.5 Summary.....	12
2.3 TPM for IMPS Design Philosophy.....	12



<b>Accession For</b>	
NTIS GRA&I	<input checked="" type="checkbox"/>
DTIC TAB	<input type="checkbox"/>
Unannounced	<input type="checkbox"/>
Justification	
By	
Distribution/	
Availability Codes	
Dist	Avail and/or Special
A-1	

3.0	DESIGN PROGRESS.....	15
3.1	General Instrument Design.....	15
3.1.1	System Configuration.....	15
3.1.2	Isolation and Grounding.....	17
3.2	Sensors.....	20
3.2.1	E-field Sensor Types.....	20
3.2.2	TPM for IMPS E-field Sensor.....	22
3.2.3	Current Sensors.....	25
3.2.4	Remaining Sensor Issues.....	27
3.3	Central Processor.....	27
3.3.1	Pulse Analyzer.....	29
3.3.1.1	Peak Amplitude Detector.....	29
3.3.1.2	Peak Derivative Detector.....	32
3.3.1.3	Pulse Integral Detector.....	32
3.3.1.4	Pulse Counter.....	36
3.3.1.5	Pulse Analyzer Performance Summary.....	36
3.3.2	TPM/TIS Interface.....	36
3.3.2.1	TPM/TIS Interface Definition.....	36
3.3.2.2	TPM Interface Circuitry.....	38
3.3.2.3	Interface Software.....	42
3.3.3	Power Supply.....	48
3.3.4	Mechanical Design.....	50
3.4	Ground-Support Equipment.....	52
3.4.1	TIS Emulator Hardware.....	53
3.4.2	Software.....	53
3.4.3	Calibration Stimulus.....	53
4.0	PERFORMANCE SUMMARY.....	56
	REFERENCES.....	R-1

## ILLUSTRATIONS

1	Technical Considerations in Spacecraft Charging.....	6
2	Engineering View of Interference Control Problem.....	12
3	TPM Description.....	16
4	TPM General Configuration on IMPS.....	16
5	TPM Configuration on IMPS.....	17
6	TPM Configuration on PASP Experiment.....	18
7	PASP/Sensor Interface.....	18
8	Isolation and Grounding.....	19
9	Approaches to Transient Field Sensor Design.....	21
10	Equivalent Circuits of Small Electric Dipole.....	23
11	Electric-Field Sensor Configuration and Schematic.....	24
12	SPM/Sensor Interface Details.....	25
13	TPM Current Sensor.....	27
14	TPM Functional Block Diagram.....	28
15	Central Processor Configuration.....	30
16	TPM Waveform Characterization.....	31
17	Proposed TPM Peak Amplitude Detector.....	31
18	TPM Peak Detector Response.....	32
19	Proposed TPM Peak Derivative Detector.....	33
20	TPM Rate-of-Rise Detector Response.....	33
21	Proposed TPM Pulse Integral Detector.....	34
22	TPM Integral Detector Response.....	35
23	TPM/TIS Interface.....	37
24	Timing Diagram.....	38
25	TPM/TIS Interface Block Diagram.....	39
26	TPM/TIS Digital Interface.....	40
27	Overall Program Flow.....	44
28	TPM Packet Structure.....	47
29	Power Supply Schematic.....	49

30	Power Profile.....	50
31	Box Design.....	51
32	GSE Hardware and Control Monitor Functions.....	52
33	Control Monitor GSE: Text Display.....	54
34	Control Monitor GSE: Stripchart Display.....	54
35	GSE Hardware, Sensor Stimulus Configuration.....	55
36	Sensor Stimulus Sample Waveform.....	55

## TABLES

1	CT-2 Characteristics.....	26
2	Measurement Ranges.....	56
3	Carrier Resources.....	57
4	Temperature Requirements.....	57



## GLOSSARY

A/D	analog-to-digital
AFGL	Air Force Geophysics Laboratory
AFWAL	Air Force Wright Aeronautical Laboratory
BCE	bench checkout equipment
CDR	Critical Design Review
CDS	circuit data sheets
E-field	electric field
EMI	electromagnetic interference
EMP	electromagnetic pulse
EO	electro-optical
ESL	Electromagnetic Sciences Laboratory (SRI)
ETS	electrical transient sensor
EWG	Experimenters' Working Group
FACC	Ford Aerospace & Communications Corporation
FET	field-effect transistor
FMEA	failure modes effects analysis
GSE	ground-support equipment
ICD	Interface Control Document
IMPS	Interaction Measurement Payload for Shuttle
IRD	Investigation Requirements Document
IR&D	internal research and development
JPL	Jet Propulsion Laboratory
MAC	months after (contract) commencement
PASP	Photovoltaic Array Space Power (Experiment)
PDR	Preliminary Design Review
PFR	Problem/Failure Report
PPL	Preferred Parts List
PROM	programmable read-only memory

PSR	Project Status Report
RFP	Request for Proposals
R&QA	reliability and quality assurance
SPAS	Shuttle Pallet Satellite
SPM	Surface Potential Monitor
STS	Space Transportation System
TIS	TPSP Interface System
TPM	transient pulse monitor
TPSP	Transient Pulse and Surface Potential (Investigation)
TRSF	Test Results Supply Form

## 1.0 INTRODUCTION

### 1.1 The IMPS Program

Designers of spacecraft and space systems must take into consideration the effects of the space environment to evolve designs capable of functioning satisfactorily in this environment. To achieve this goal, it is necessary to understand both the environment and the system's interactions with it. Sounding rockets and scientific satellites have been used to obtain information regarding the environment, and laboratory experiments and simulations have increased our understanding of the relevant interactions. This experimental work has been complemented by the development of analytical models that guide design evolution. Feedback from operational systems has been used to refine our understanding of the environment and its interactions with the systems and to verify the appropriateness and adequacy of design procedures.

Periodically, events occur that require a special program of investigation. Such a program is the Interaction Measurements Payload for Shuttle (IMPS), which is responding to the confluence of two recent developments: current plans for large space structures, and recently available data regarding the polar orbital environment.

Large space structures incorporating substantial areas of dielectric material and new generation solar cells are currently being planned. These systems will operate in polar orbits, where recent work by the Air Force Geophysics Laboratory (AFGL) [Gussenhoven et al., 1985] indicates that, under auroral conditions, electrostatic charging of the sort commonly observed at synchronous orbit may occur. Since the design and assembly of a large space system is costly, it is important that potential problems be addressed carefully with adequate lead time to permit the results to be incorporated into the designs.

Although the problem of satellite interactions with the environment has historically been treated by means of analysis and laboratory simulation supplemented by feedback from operational vehicles, two important considerations have led to a departure from this general approach in the IMPS program. First, the Space Transportation System (STS) (shuttle) is available to carry experiments to orbits of interest. Second, the cost of a large space system is so great that it is imprudent to rely entirely on analytical and laboratory work to guide the designs. Thus, the IMPS program is based on the development of a suite of instruments that can be orbited on several missions to obtain critical information regarding the interaction of space systems with their orbital environment. This information will be used to develop systems that can perform their missions with a high confidence of success.

## 1.2 Role of the Transient Pulse Monitor

One important interaction between a space system and its orbital environment is the deposition of electric charge at various depths within the materials composing the system. A potential consequence of this non-uniform charge deposition (differential charging) is the occurrence of discharges. High voltage in the system may aggravate this effect. These discharges produce a number of effects, including transient electromagnetic fields in their vicinity which, in turn, induce currents and voltages in system circuitry. To properly assess the threat posed by electrostatic charging and discharging to a given system, it is necessary to detect these events and to quantify the important electrical and electromagnetic properties that affect system performance.

This is precisely the motivation behind the Transient Pulse Monitor (TPM) planned for the IMPS mission. The TPM will monitor the occurrence and record the waveform characteristics of any discharges.

To achieve the goals of the TPM, one might wish to orbit an oscilloscope or its equivalent, a digital transient recorder in order to record the transient electromagnetic signals generated as a result of the space systems interaction with the ambient plasma environment. Unfortunately,

the speed of the discharges (in the laboratory, rise times of a few nanoseconds have been observed) is such that a modern wideband oscilloscope or its equivalent (a transient digitizer) would be required for each of the sensors used in the experiment. The size, weight, and power restrictions imposed on satellite experiments make this approach impractical. Thus, other methods for pulse characterization must be developed. SRI has evolved a system for pulse characterization that measures the critical time-domain parameters of the electromagnetic pulses of interest (e.g., peak amplitude, rise time, integral, and pulse count). In general, these are the parameters that an engineer or analyst would deduce from an oscillogram and would apply to system design and in developing subsystem procurement specifications. SRI's TPM is designed to provide this information about the transient electromagnetic signals observed on a satellite.

The multichannel TPM developed by SRI can be built to monitor the transient electromagnetic signals generated simultaneously in an arbitrary number of sensors. Six sensors will be employed for the IMPS mission. SRI's TPM design is such that the choice and placement of the sensors can be adjusted at any time without affecting the TPM. This allows great project/mission flexibility, since the TPM design and fabrication that requires the greatest lead time can be undertaken immediately, while sensor choice and placement, which may require repeated meetings with affected experimenters, can occur later in the project schedule.

Thus, the TPM can achieve several important goals: It can allow the unequivocal detection of discharges at specific locations and correlate them with other events in time. In addition, it can characterize important features of the discharges to help quantify the electromagnetic threats to satellites in orbit. Such information is essential to assess the most efficient hardening techniques to be applied to a system to achieve the desired immunity against the effects of the orbital particle environment. Finally, these basic orbital data can be compared with the results of analyses and laboratory simulations of discharging to ensure that the results of analysis and simulation agree with orbital experience. In this way, design changes suggested in the laboratory can be

applied to spacecraft with high confidence that the designs will also work in orbit.

## **2.0 BACKGROUND**

### **2.1 Experimental Studies**

Spacecraft charging to large potentials was first reported by DeForest [1972], and the discharging resulting from differential charging was first detected on an orbiting satellite by Nanevicz, Adamo, and Shaw [1973] of SRI. Since that time, however, the study of charging processes and their effects on satellites has proceeded unevenly, largely because experiments on satellites are substantially more difficult than laboratory experiments. Thus, since the synchronous orbit experiments on DSP-4 of Nanevicz et al. [1975], only the P78-2 (SCATHA) satellite [Stevens and Vampola, 1978] has been instrumented specifically for the in-orbit study of spacecraft charging. In the interim, experimental activity has focused on laboratory experiments [Adamo and Nanevicz, 1976; Stevens et al., 1977] and on the development of improved simulation techniques [Nanevicz and Adamo, 1977; Adamo and Nanevicz, 1983].

A further reason for the uneven development of a more complete understanding of spacecraft charging is that the overall problem has several facets that may legitimately be studied independently. The principal technical considerations in spacecraft charging and their roles (Figure 1) are summarized below.

#### **2.1.1 Orbital Particle Environment**

A description of the particle types and their energies present during an electron injection event is important on a scientific basis and because it provides insight into what may be required to properly simulate the space environment in the laboratory; i.e., it provides the "source terms."

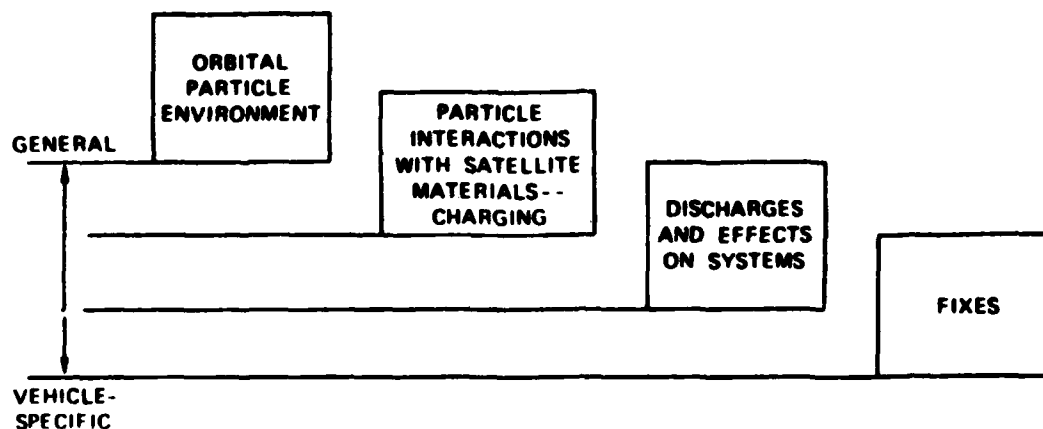


Figure 1. Technical Considerations in Spacecraft Charging.

#### 2.1.2 Particle Interactions with Satellite Materials: Charging

Proven techniques to account for and quantify the electrical behavior of aggregates of conducting and insulating materials in the ambient particle environment are important in predicting available stored energies and behavior of specific materials. Also of interest is direct ionization by extremely energetic particles.

#### 2.1.3 Discharges and Their Effects on Systems

Knowing which spacecraft materials are responsible for charging and understanding the characteristics of the discharges from these materials allows the designer to choose between several alternatives, such as:

- Avoiding the use of susceptible materials
- Altering the charge/discharge characteristics of materials
- Controlling their placement
- Electromagnetically hardening the satellite to render it immune to the effects of the discharges.

In addition, information on the properties of the discharges occurring in space is essential for developing and validating schemes for simulating



spacecraft charging in the laboratory, and for developing military standards and specifications.

#### **2.1.4 Fixes**

Ultimately, the space system designer must combine the information on the effects of vehicle/environment interactions to develop designs and manufacturing techniques to enable the system to function satisfactorily in space.

### **2.2 Current Understanding of the Technical Areas**

#### **2.2.1 Orbital Particle Environment**

The study of this area is fundamental in that, conceptually, it simply involves carrying sensors designed to sample and characterize the particle environment existing at the orbits of interest. In practice, great care is necessary to ensure proper calibration of the sensors and to minimize and account for the effects caused by the presence of the satellite and its sensors. Thus, as indicated at the left of Figure 1, the results are very general, in that they describe the naturally occurring environment in space, and, if done properly, they are independent of the specific satellite used for the measurement. In general, this facet of the space investigation is closest to pure science, and the techniques appropriate for its study are well developed. Indeed, it is intended that IMPS will carry a set of instruments to define the ambient particle environment during the experiments.

#### **2.2.2 Particle Interactions with Satellite Materials: "Surface" Charging**

Spacecraft charging may in general be divided into two broad categories: surface and deep. Surface charging occurs when charged particles impinge on the outermost surface material of a vehicle and lose all their kinetic energy before penetrating the surface. They are trapped in the surface layer of material.

Deep charging occurs where the impinging charged particles have sufficient energy to penetrate past the surface layer and become logged in materials deep within the structure. This area is more material- and design-specific, since it involves satellite material properties as well as the characteristics of the environment.

The surface problem has been studied in the laboratory, beginning with the studies of Adamo and Nanevich [1976] and continued by Stevens et al. [1977] and many others. Analytical studies were carried out by Katz et al. [1977], culminating in the NASCAP code for predicting charge accumulation on various satellite surfaces. Unfortunately, orbital experiments to verify the validity of the laboratory work and analyses have been few. Data from the SCATHA satellite reported by Mizera et al. [1981] verified the general behavior observed in the laboratory studies with modulated illumination [Adamo and Nanevich, 1979]. Laboratory work by Adamo and Nanevich [1977] indicating that Kapton should become progressively more conducting (and less able to store charge) with exposure to sunlight in orbit has been verified by experiments on SCATHA, as reported by Vampola [1980]. The SCATHA satellite carried provisions for the study of the charging behavior of a carefully selected set of material samples, probably the largest set that can practically be accommodated on a single satellite experiment.

The motivation to study the interaction problem on IMPS is strong, since planned space systems will:

- Be exposed to new environments
- Employ new materials in new configurations
- Employ new operating conditions (e.g., higher voltages on the solar arrays).

These considerations, coupled with the rather sparse orbital information presently available specifically on interactions at low polar orbit, have led to the inclusion of interaction experiments on the IMPS payload.

### 2.2.3 Discharges and Their Effects on Systems

This problem is substantially more vehicle-specific and probably less well understood at this time, since it presupposes an understanding of the environment, how it deposits charge in satellite materials, and how a discharge is triggered and propagates. In general, when sufficient charge is stored in a material, a discharge will be triggered at some place in the material. The discharge propagates, tapping the stored charge, causing currents to flow, and generating plasmas, all of which combine to produce an electromagnetic pulse (EMP), either radiated, conducted, or both.

The properties of these pulses were first studied in the laboratory by Adamo and Nanevich [1976] in connection with the development of instrumentation for the DSP-4 satellite measurement project [Nanevich et al., 1975]. Later, they studied the electromagnetic signals generated by discharges in a special "electromagnetically clean" apparatus in the laboratory [Nanevich et al., 1980].

The instrumentation on the P78-2 SCATHA satellite periodically measured the transient pulse signals induced in a short dipole antenna at the end of a 2-meter-long boom on the exterior of the satellite [Stevens and Vampola, 1978]. The sophisticated time-sampling instrumentation used for this measurement allowed only one processor to be included in the SCATHA payload. Hence, it could not be dedicated to the study of external fields, but spent three-quarters of its available time monitoring signals existing at three points on the interior of the satellite. This lack of continuous information about the external environment limited our ability to compare internal system responses to external EMPs.

Since P78-2 SCATHA carried only one sensor to measure the exterior transient electromagnetic environment, it was not possible to use schemes such as amplitude triangulation to estimate where on the exterior of the satellite a discharge occurred in order to infer absolute discharge source strength from the data. Also, locating the external transient sensor at the end of the boom on SCATHA introduced additional ringing in the received signal. In our design for the TPM instrumentation and sensor installation on IMPS, we have benefited from the experience gained on

SCATHA, DSP-4, and in the laboratory to maximize the technical yield from the experiment.

The problem of coupling transient EMPs into systems is not unique to spacecraft charging. Coupling problems arise when assessing system vulnerability to other transient signals, such as lightning and the clear EMP, and a great deal of work has gone into the study of these problems. In general, it is found that coupling is critically dependent on the design details of the system in question (design of shields, treatments applied to penetrating conductors [such as wires and cables], and aperture treatments), as well as upon the physical location and electromagnetic properties of the source. For example, low frequencies enter a system most readily along penetrating electrical conductors, while high frequencies can propagate easily through apertures in the shield structure.

For the case of spacecraft surface charging and discharging, the electric fields induced on the spacecraft exterior will have characteristics that include both the source waveform and damped oscillations with frequencies associated with the lengths of metal structural elements. The resulting internal transients will typically be damped oscillations with frequencies associated with wiring lengths and system impedances (termination, mutual, and parasitic impedances). For space structures appropriate to the IMPS program, the external resonances will be of the order of a few tens of megahertz, and the internal resonances will be scattered throughout the range 20 MHz to 100 MHz. Pulse durations will typically be shorter than a few microseconds.

The TPM under development by SRI provides data outputs that characterize these pulses. These outputs include:

- Peak pulse amplitude (positive and negative peaks)
- Peak pulse derivative (positive and negative rates of rise)
- Integral of the absolute value of the pulse (rectified impulse)
- Number of such pulses per unit time that occur at each sensor.  
There is considerable flexibility in the unit chosen.

These outputs will aid in refining our understanding of the external discharge process and its effect on internal subsystems. This will provide a data base that can be used to:

- Better understand the physics of discharges
- Quantify differences between space environments
- Develop specifications and standards for the procurement of materials, components, and subsystems
- Develop more realistic laboratory simulations and standard test procedures
- Provide information on the behavior of specific elements, such as the Photovoltaic Array Space Power (PASP) experiment, planned for use on large space systems.

When SCATHA was launched, much of the spacecraft community hoped that it would provide substantially complete answers to most of the questions concerning charged-particle interactions with spacecraft. Many questions were answered, but as is often the case in scientific investigation, as many new questions were posed. At recent meetings on the topic of spacecraft anomalies, debate on charged-particle/spacecraft interactions and their effects on systems has heightened. Of special concern are large-space-structure interactions with the low-Earth, polar environment. These debates have revealed the need for data obtained in orbit.

#### 2.2.4 Fixes

The general interference control problem is shown in Figure 2. A source of electromagnetic interference exists, and interacts with a victim system via one or more coupling paths. The degree to which the designer must be concerned with this problem depends upon the strength of the source, the susceptibility of the victim, and the character of the coupling path.

Since the severity of the overall problem depends upon the properties of these three principal elements, immunity can be ensured by:

- Eliminating the source
- Controlling the coupling
- Hardening the victim.

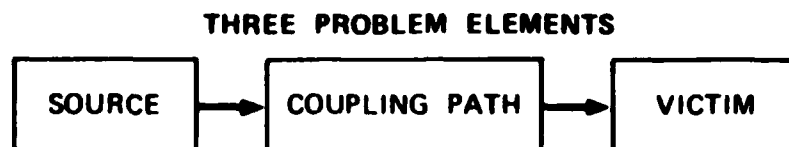


**Figure 2. Engineering View of Interference Control Problem.**

An efficiently engineered solution requires information on each of the major elements. In particular, the properties of the source are critical, since they establish the levels and frequency characteristics that must be considered in the design.

#### **2.2.5 Summary**

The experience SRI has gained in studying charged-particle interaction with spacecraft and the resultant discharge characteristics, both in orbit and in the laboratory, is being applied to develop TPM sensors and an instrumentation system for the IMPS program designed to yield the data most relevant to the future development of large space systems.

#### **2.3 TPM for IMPS Design Philosophy**

As indicated in more detail in Section 3.0, the TPM project is concentrating on the development and integration of a TPM instrument for the IMPS program.

The TPM package has been designed to respond to the needs of the IMPS program and to take advantage of SRI's continual involvement in spacecraft charging studies since 1973. This activity has included laboratory

studies, as well as the design and conduct of orbital experiments. SRI's Electromagnetic Sciences Laboratory has used its own funds to supplement contract funds to (1) maintain continuity in its involvement in this area, particularly in the development of laboratory simulation techniques and in the improvement of circuits suitable for orbital measurements, and (2) capitalize on the latest electronic technological developments.

The TPM system provides information necessary in quantifying and coping with electrical discharges stemming from spacecraft interaction with its orbital environment. Basically, the TPM system consists of a central processor that accepts simultaneous inputs from six electromagnetic sensors. The output from the central processor is a series of numbers describing the key properties (peak amplitude, maximum rate of rise, integral, and repetition rate) of each of the six transient signals measured, along with indications of the instrument's state of health.

The central processor accepts signals from a variety of sensors (in this regard, it is similar to a multichannel oscilloscope). The output from each basic processor channel is an analog signal that is proportional to the quantity being measured. These basic outputs are processed by a digital system, forming part of the processor, and translated into a digital data stream compatible with the data formats planned for the IMPS payload.

The TPM central processor channels are housed in a single package. Power and telemetry output connections are made using standard satellite cabling techniques. The TPM system is designed to accommodate signals observed in laboratory simulations, with rise times as short as a few nanoseconds. Accordingly, the input circuitry requires coaxial cable connections to the sensors.

To achieve maximum flexibility in the types of possible measurements, the TPM system will be supplied with a mixture of electric field (E-field) and current sensors. This approach allows the study of both radiated fields on the surfaces of the payload, as well as transient currents induced on selected wiring on the satellite. Present plans call for one

electric-field sensor to be monitored near the PASP array trays and one current sensor to monitor the main high-voltage lead of the PASP experiment.

At present, a carrier (satellite) has not been identified for the IMPS mission, nor has a configuration of the experiments been defined. Thus, it is difficult to fully identify the exact measurement objectives and sensors to be used in the TPM.

Fortunately, the choice of sensors and their placement on the selected carrier will not materially affect the TPM design. Thus, we anticipate that time will be available to precisely define the sensors in close cooperation with the eventual experimenters, thereby ensuring an optimum arrangement. Current plans call for the construction of six E-field sensors and one I sensor.

The equipment needed to exercise and calibrate the TPM system has been built as a prototype, and an operational unit will be provided as part of the ground-support equipment (GSE) package. The TPM requires no special in-flight conditioning or calibration. The circuits are inherently stable, so that no trimming adjustments are needed. System function will be verified at each phase of test and integration, and the GSE exercises the TPM system completely.



### 3.0 DESIGN PROGRESS

#### 3.1 General Instrument Design

The TPM instrument for IMPS has grown out of SRI's continued involvement in spacecraft charging studies. SRI has been at the forefront of the study of spacecraft charging since its discovery. The TPM for the IMPS mission represents the evolutionary development of the instrument that SRI flew on SCATHA in 1978. We have since improved the performance of its critical circuits in almost every regard. It is now able to capture the salient features of extremely fast electromagnetic transients (rise times of a few nanoseconds).

During the preliminary design phase, SRI's existing and prototype TPM designs were adapted, and new interface circuit designs were defined to satisfy the needs of the IMPS mission. This effort included design of the electrical interface with the Surface Potential Monitor (SPM) through the Transient Pulse/Surface Potential Monitor Interface System (TIS) (power, telemetry, commands, and cabling); design of the mechanical interface between the TPMs transient E-field sensors and the SPM's sample trays; design of the electrical and mechanical interface between the TPM's sensors and the PASP experiment; and finally, design of the electrical, mechanical, and thermal interfaces between the TPM and the proposed carrier, SPAS.

##### 3.1.1 System Configuration

The TPM is a self-contained unit housing all pulse analysis, power conditioning, and command/telemetry circuitry in a central processor while transient events are detected by six remotely mounted sensors (Figure 3). Sensors are of two types: those that respond to radiated electromagnetic signals, and those that respond to conducted signals. The TPMs central processor will be mounted along with the SPM experiment on a single SPAS pallet on the upper face, extreme end of the vehicle (Figure 4). Two

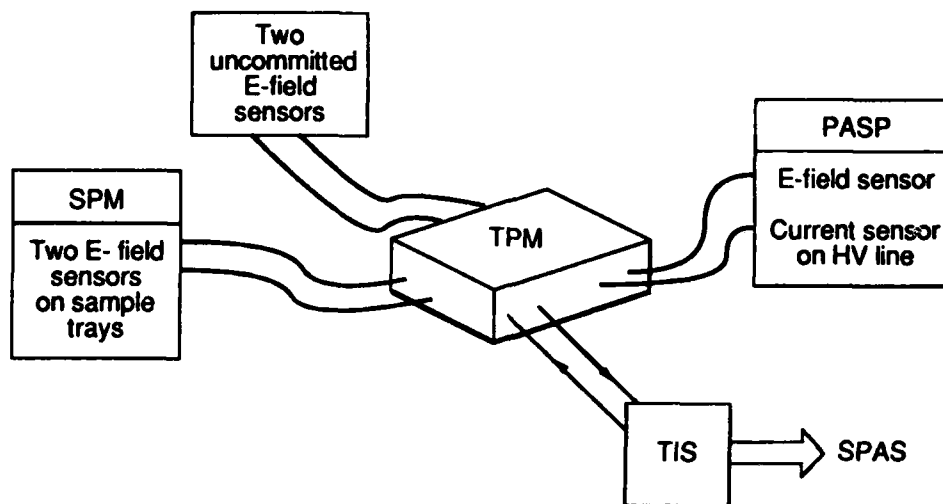


Figure 3. TPM Description.

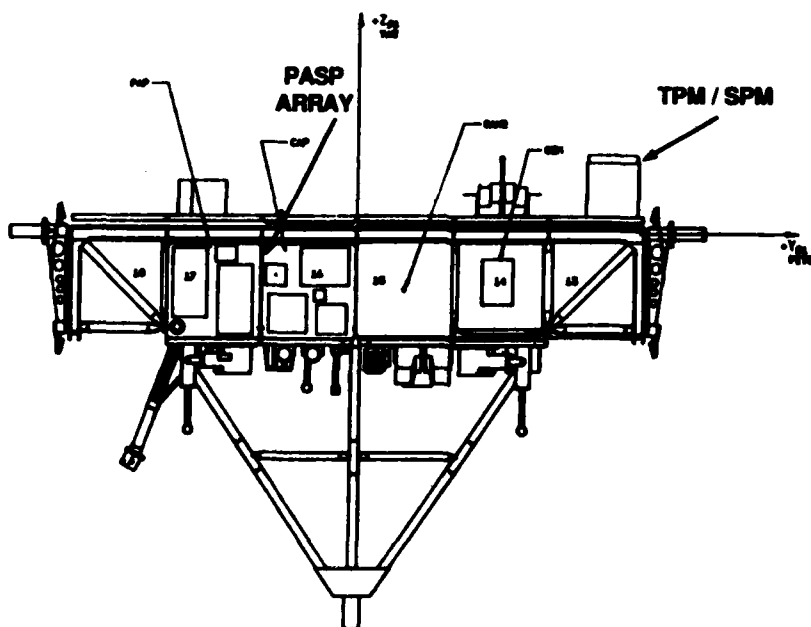
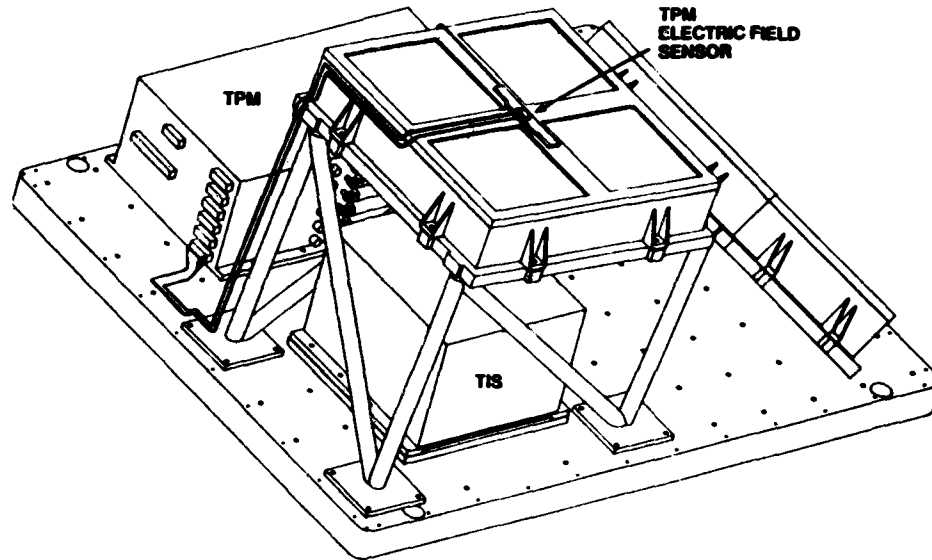


Figure 4. TPM General Configuration on IMPS.



**Figure 5. TPM Configuration on IMPS.**

radiated electromagnetic signal sensors will be mounted on the two SPM sample trays (Figure 5). Two TPM sensors will monitor for transients in the PASP experiment, and one conducted sensor will be placed on the high-voltage bias supply connection to the test solar array panels. One radiated electromagnetic signal sensor will be placed on one of the solar array panels (Figures 6 and 7).

The remaining four sensors will detect the radiated electromagnetic signals. Their placement and measurement objectives are not yet determined. We have standardized a particular design (described in Section 3.2.2) that is suitable for PASP and are constructing five more of this type (transient E-field).

### **3.1.2 Isolation and Grounding**

The TPM system, with one exception explained below, is designed to isolate the circuits from their enclosures and the carrier chassis (Figure 8). Power is transmitted to the E-field sensors via shielded twisted pairs with discrete returns (the current sensors do not require

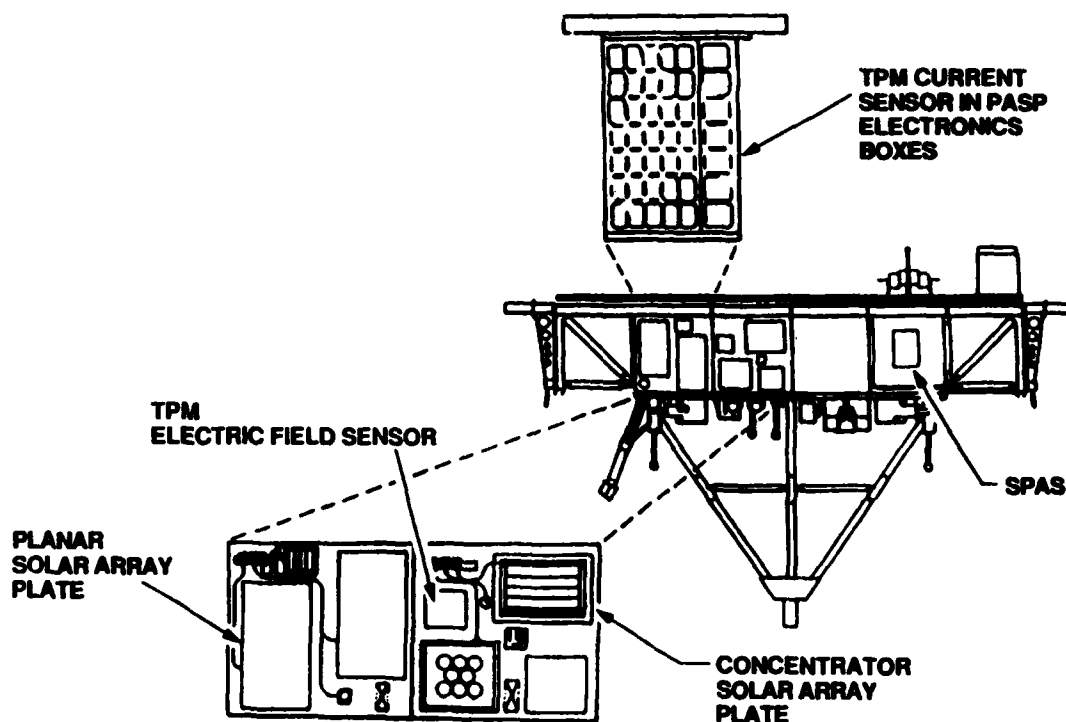


Figure 6. TPM Configuration on PASP Experiment.

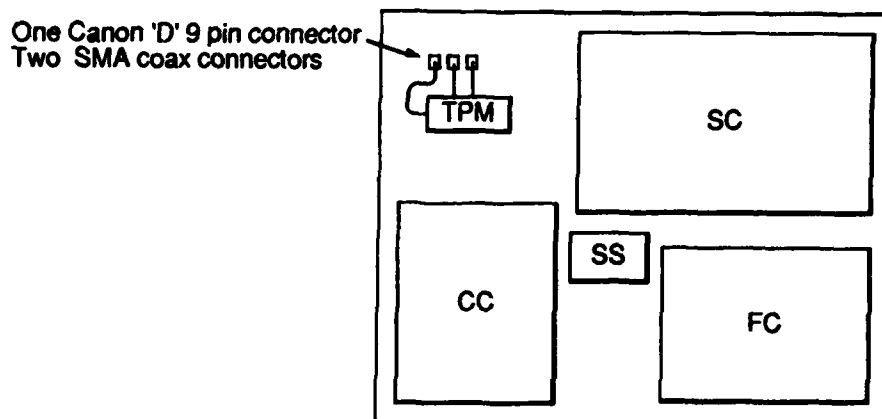


Figure 7. PASP / Sensor Interface.

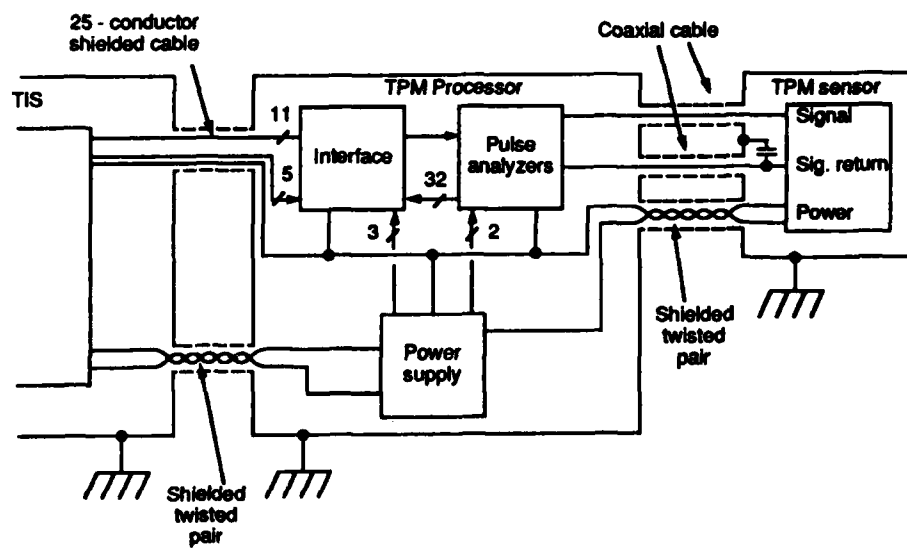


Figure 8. Isolation and Grounding.

power). Each analog signal and signal return is carried on a separate coaxial cable. The digital signals to the TIS are carried on a 25-conductor shielded cable. Shields on all the cables are connected to the TPM enclosures, but isolated from the circuits, for highest shielding effectiveness.

One variance from the isolation specification is required for operation of the E-field sensors. To measure the true electric field at the sensor location, it must have a low-impedance connection to the sensor housing in the frequency range of interest. To fulfill this operational requirement, we must install a capacitive connection from the sensor circuit to the sensor housing. This variance has been approved by the project.

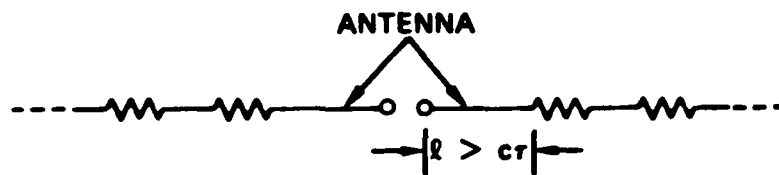
### **3.2 Sensors**

The two sensor types to be used on the IMPS are: five active E-field sensors to measure transient electric fields radiated by a discharge, and one passive current transducer to record transients induced on the high-voltage supply cable of the PASP experiment.

#### **3.2.1 E-field Sensor Types**

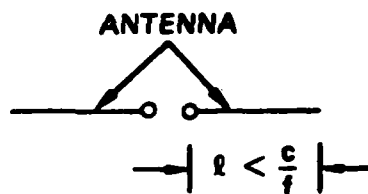
SRI has used several types of E-field sensors (such as long wires, rotating-vane and vibrating-reed field meters, and passive metal plates) to measure static charging effects in the laboratory and on aircraft, missiles, and spacecraft.

When designing a field sensor to characterize spacecraft discharges, it is important to recognize that a discharge caused by spacecraft charging is a brief phenomenon; excessive distortion of the transient data by successive reflections from the ends of the sensing antenna (ringing) must be prevented. Two possible solutions to this problem are illustrated in Figure 9. First, the sensor element may be made so long that the relevant portion of the transient signal is recorded before the reflection from the end of the sensor returns (Figure 9a). To minimize reflections, the far end of the sensor may be made lossy and may be terminated in its



where  $c$  = velocity of light  
 $t$  = transient duration

**(a) USE OF LONG ANTENNA TERMINATED IN LOSSY MATERIAL TO INHIBIT REFLECTIONS**



where  $c$  = velocity of light  
 $f$  = upper frequency limit  
of recording system

**(b) USE OF SHORT ANTENNA SYSTEM--RINGING OCCURS ABOVE HIGHEST FREQUENCY RECORDED**

**Figure 9. Approaches to Transient Field Sensor Design.**

characteristic impedance. As a second solution, the dimensions of the sensor may be made electrically small so that the first sensor resonance occurs above the highest frequency of interest (Figure 9b) and will not distort the measurement. Although large antennas can be considered for the ground-based study of transient signals, only electrically small sensors are practical for in-flight measurements.

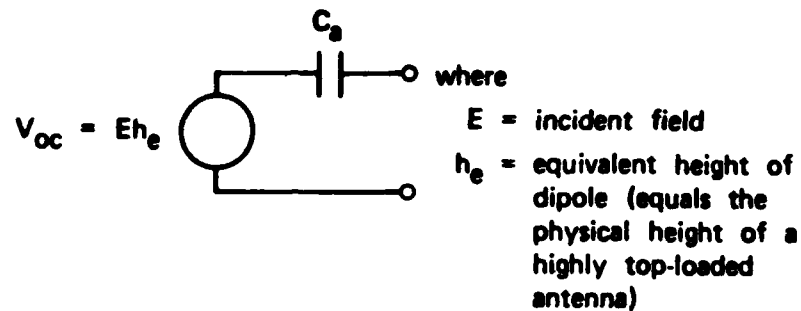
The electrically small field sensor output can be made proportional to the electric field or its derivative at the sensor's location. Equivalent circuits for the small electric dipole are shown in Figure 10. The open-circuit voltage of the electric dipole is directly proportional to the local electric field (Figure 10a); the short-circuit current is proportional to the derivative of the electric field (Figure 10b). The short-circuit current can be measured using a broadband current transformer. With modern high-impedance field-effect transistor (FET) input amplifiers, the open-circuit voltage can be measured over a wide range of frequencies.

### **3.2.2 TPM for IMPS E-field Sensor**

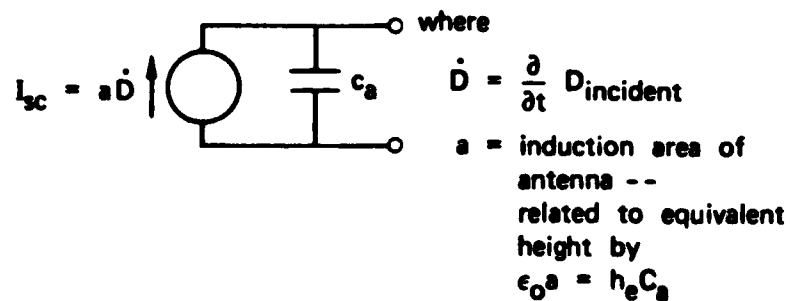
For the IMPS TPM system, we employ a small electric dipole with a built-in FET preamplifier, so that the open-circuit voltage (proportional to the E-field normal to the sensor) is measured. A unit as designed for the SPM is shown in Figure 11. The antenna itself is a circular metal plate that is dielectrically mounted on a small box containing the preamplifier circuit. The preamplifier housing is designed to fit conveniently on an SPM sample tray. Figure 12 shows the details of the SPM interface. This configuration is quite rugged and compact, occupying about 100 cm<sup>3</sup>. The sensor design can respond to frequencies as high as several gigahertz, well in excess of the range required for the specified transients. The preamplifier drives a balanced 50  $\Omega$  coaxial line leading to the central processor.

The preamplifier circuit is designed to accommodate a wider thermal tolerance specification than the TPM central processor electronics, but will undergo the same R&QA, testing, calibration, etc. The thermal





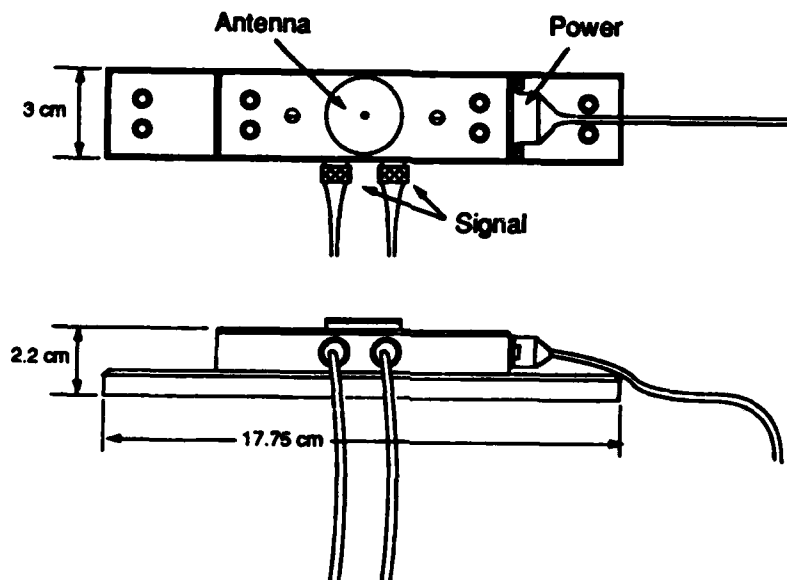
(a) THEVENIN EQUIVALENT CIRCUIT OF ELECTRIC DIPOLE



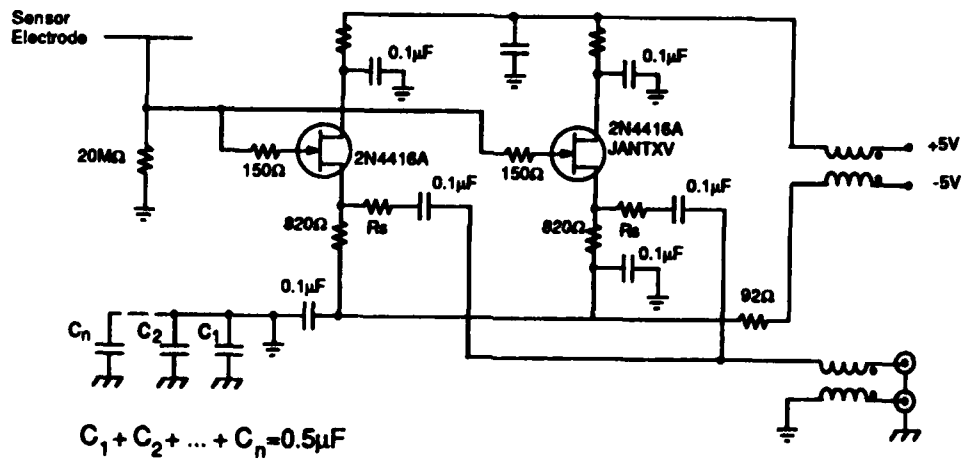
(b) NORTON EQUIVALENT CIRCUIT OF ELECTRIC DIPOLE

Figure 10. Equivalent Circuits of Small Electric Dipole.

**a. Configuration**



**b. Schematic**



**Figure 11. Electric-Field Sensor Configuration and Schematic.**

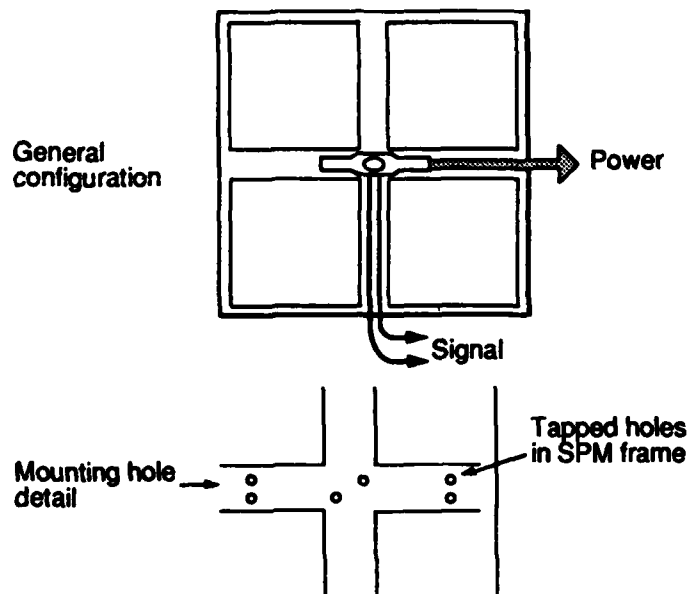


**Figure 12. SPM / Sensor Interface Details.**

interface between the sensor and its host pallets has been considered in discussions with thermal experts at JPL and has been found to be in accordance with normal JPL design practice. A schematic of the sensor is provided in Figure 11b. The preamplifier dissipates less than 0.1 W.

### **3.2.3 Current Sensors**

To sense current transients on wires, the TPM uses passive current transformers. These sensitive devices can detect over a wide frequency range without interfering with the circuits they monitor. On SCATHA, we modified the Tektronix CT-2 probe, a commercial unit whose response covers the frequency range from 1.2 kHz to 200 MHz (this accommodates pulse rise/fall times of 160  $\mu$ s to 500 ps). The unit was repackaged, fully tested, and qualified. For the IMPS measurement objectives, the Tektronix CT-2 probe again meets the performance specifications in all areas but one; the signal return does not satisfy the grounding isolation requirements. However, in repackaging the unit for flight, we converted the current sensor's operation to isolate the signal return by using a

**Table 1**  
**CT-2 CHARACTERISTICS**

Parameter	Value
Sensitivity	1 mV/mA
Accuracy	± 3%
Rise time	500 ps
Frequency response	
Low: -3 dB	1.2 kHz
High: -3 dB	200 MHz
Insertion impedance at:	
10 MHz	0.1 Ω
100 MHz	0.5 Ω
Capacitive loading barewire	1.8 pF for #16
Maximum barewire voltage	1000 V
dc saturation current:	
Current to reduce L/R by X2	175 mA
Pulse current rating*	36 A
Not to exceed:	
Ampere S product*	$50 \times 10^{-6}$
Maximum CW current	2.5 A
Cable length	42 inch
Prop delay	6.1 ns
Cable connector	BNC
Operating temperature	-25°C

\* With 50 Ω termination. Values are reduced by a factor of 2 if unterminated.

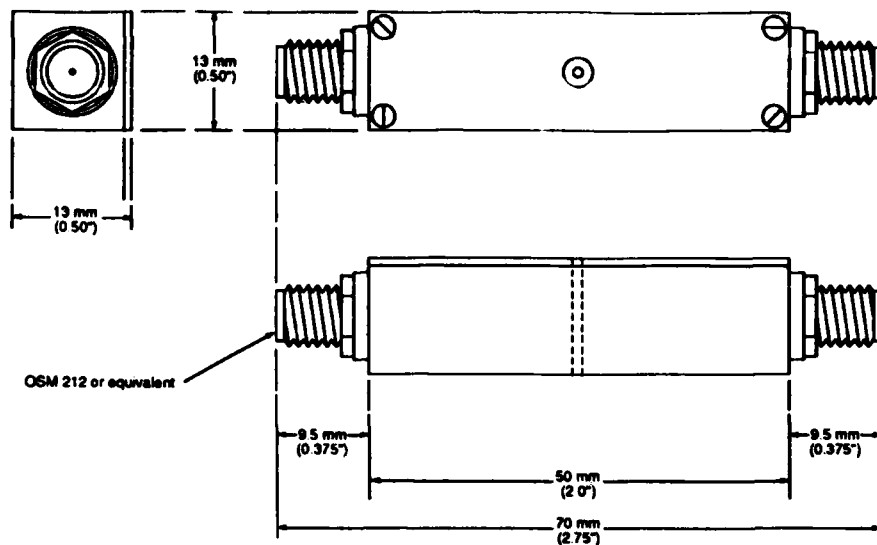


Figure 13. TPM Current Sensor.

balanced coax signal path. Performance figures for the CT-2 are given in Table 1, and the PASP current sensor is diagramed in Figure 13.

### 3.2.4 Remaining Sensor Issues

The remaining two sensors must be physically and electrically integrated with other experiments if they are to be used. The sensors are small, and their physical form and mounting configurations are amenable to a number of mounting configurations and measurement objectives. It is possible, in close consultation with eventual companion experimenters, to choose locations and configurations that will provide the most useful information about transient events without interfering with the operation of other equipment, including the monitored equipment.

### 3.3 Central Processor

The TPMs central processor is divided into sections that perform two basic functions: pulse analysis and interface (Figure 14). As shown in Figure 14, the pulse analysis section is made up from six identical boards, corresponding to the six ETS or channels. When a pulse event

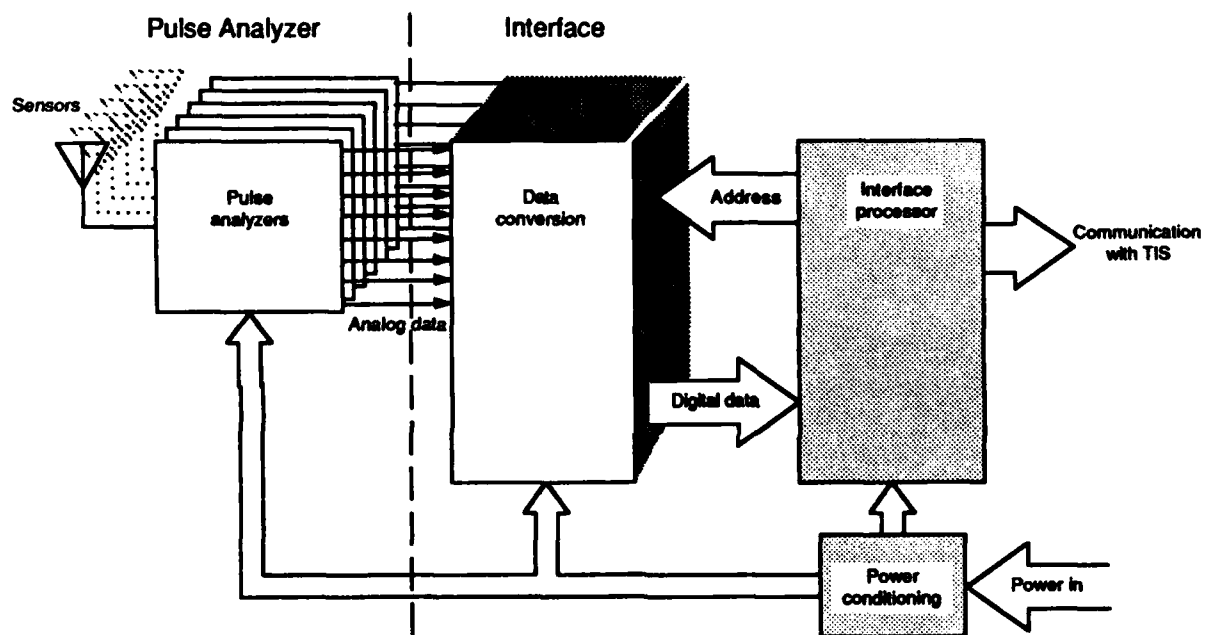


Figure 14. TPM Functional Block Diagram.

occurs, each pulse analyzer produces an array of pulse waveform parameter data in analog form. The interface circuitry addresses each analog output individually, converts it to digital form, and passes the accumulated data to the satellite (via the TIS interface).

Figure 15 shows the pulse analyzer and digital interface circuit configurations in more detail. The power supply has been omitted for clarity. The pulse analyzer shown in one of six identical circuits (channels) used to monitor six ETSs. A single digital interface addresses the outputs of all six channels, converts them to digital form, and performs all communications functions with the TIS interface, which in turn communicates with the SPAS.

### 3.3.1 Pulse Analyzer

The pulse analyzer is the heart of the central processor. It determines salient features of the transient pulses arriving from the ETS.

The signal arriving from each current or E-field sensor is buffered by a broadband amplifier and then distributed to circuits that derive the following parameters (Figure 16):

- Peak positive and negative amplitude
- Peak positive and negative derivation of pulse
- Integral (rectified impulse)
- Number of discharges within a telemetry frame.

In general, the cascade of amplifiers in the pulse analyzer circuits must have sufficient bandwidth to accommodate the important features of the discharge pulse. To achieve this bandwidth without requiring excessive power, SRI's TPM uses a discrete component design for these circuits.

#### 3.3.1.1 Peak Amplitude Detector

The peak amplitude detector (Figure 17) is based on a cascaded series of nonlinear amplifiers and peak detectors that, in combination, provide outputs proportional to the logarithm of the positive and negative input

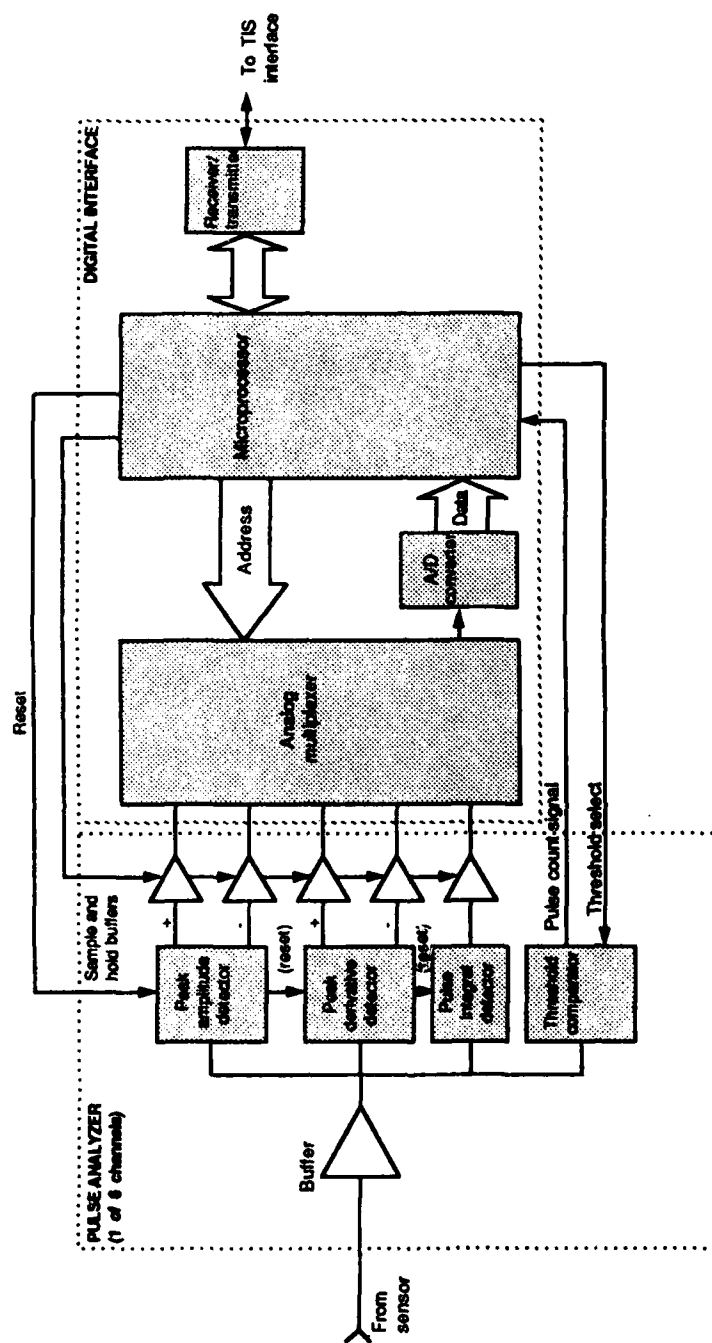


Figure 15. Central Processor Configuration.



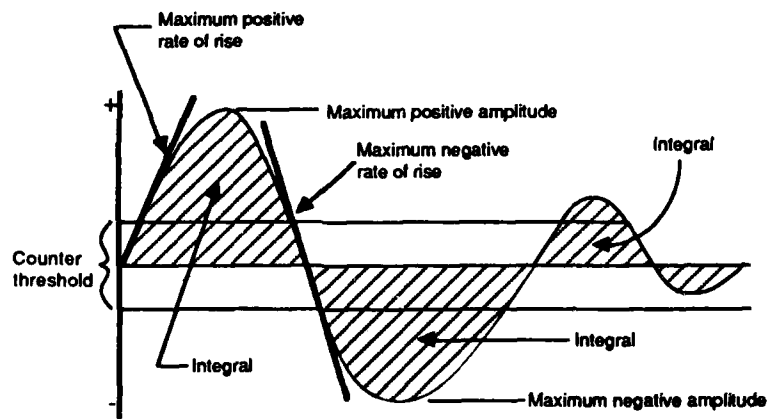


Figure 16. TPM Waveform Characterization.

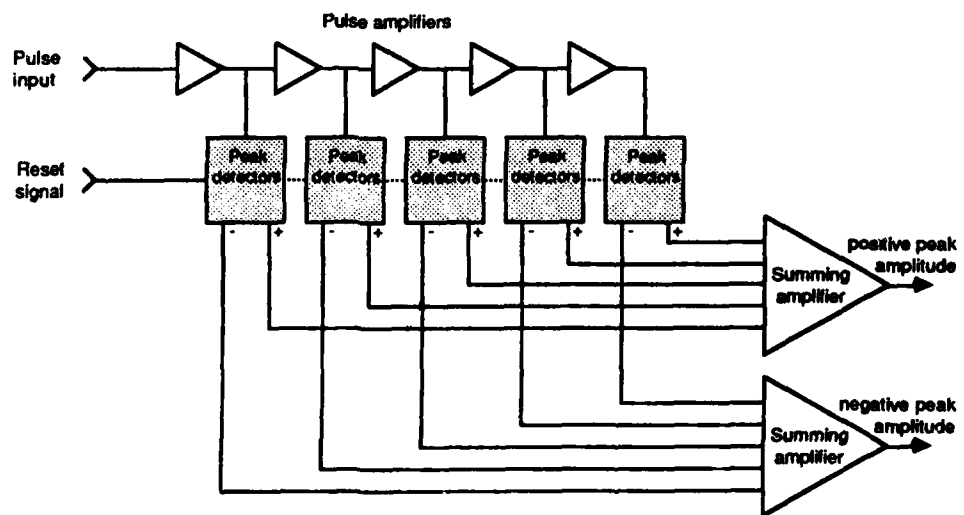
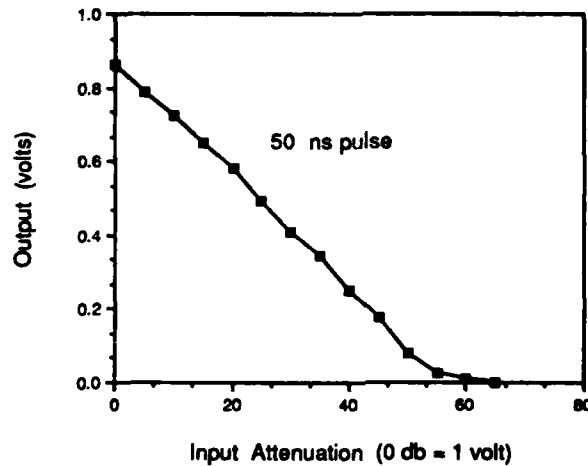


Figure 17. Proposed TPM Peak Amplitude Detector.



**Figure 18. TPM Peak Detector Response.**

maxima. This circuit architecture allows very fast pulses to be measured over a wide dynamic range with relatively little power. The proposed peak detector circuit uses five stages of amplification to attain a 60-dB dynamic range (Figure 18). Laboratory tests of the circuit show that peak values with durations as short as 2 ns can be measured.

#### **3.3.1.2 Peak Derivative Detector**

The peak derivative detector is based on a similar peak detection scheme, preceded by a differentiator circuit (Figure 19). The amplifiers and detectors have been optimized for the extremely fast signals that result from differentiation of the pulses. Laboratory tests of the circuit show that it will measure the peak derivative signals from pulses with rates of rise as fast as 0.3 ns to peak (Figure 20).

#### **3.3.1.3 Pulse Integral Detector**

The pulse integral detector has a dynamic range comparable to that of the peak detector and is similar in design approach (Figure 21). The output of the integrator is derived from the absolute value of the input.

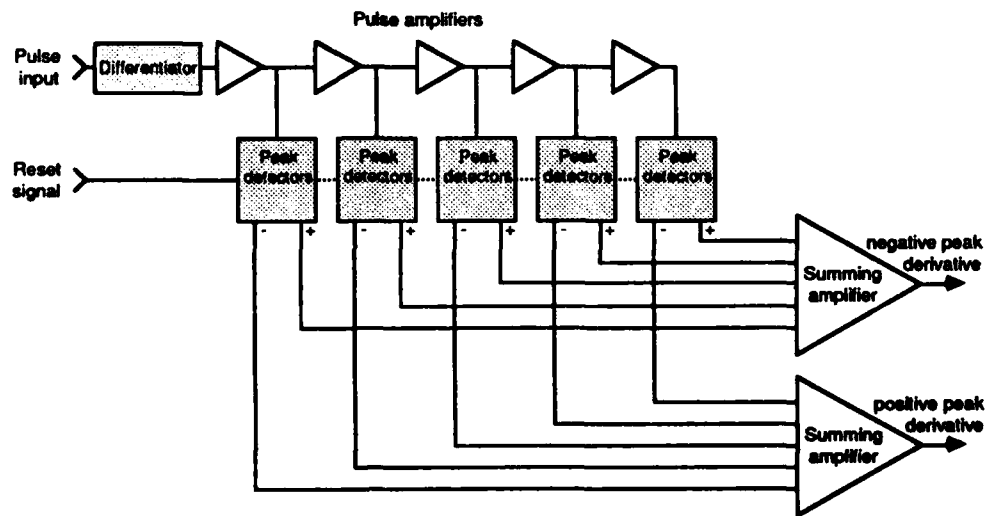


Figure 19. Proposed TPM Peak Derivative Detector.

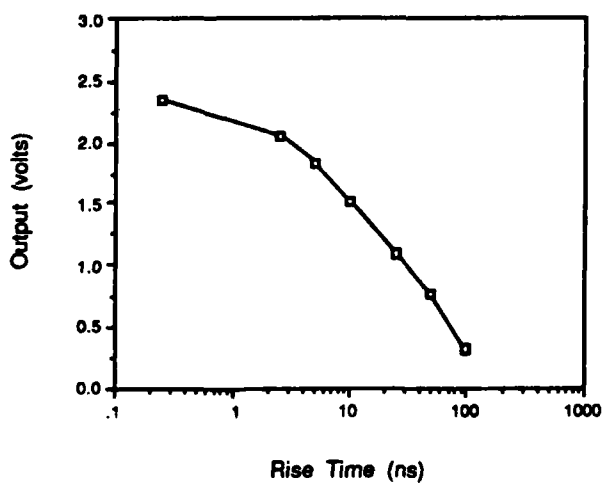


Figure 20. TPM Rate-of-Rise Detector Response.

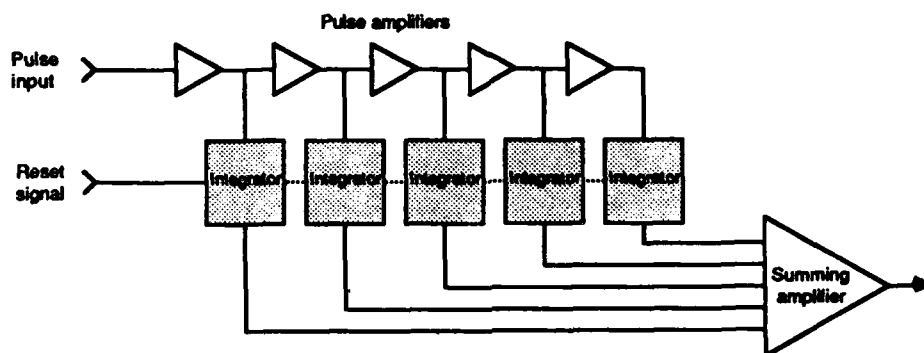


Figure 21. Proposed TPM Pulse Integral Detector.

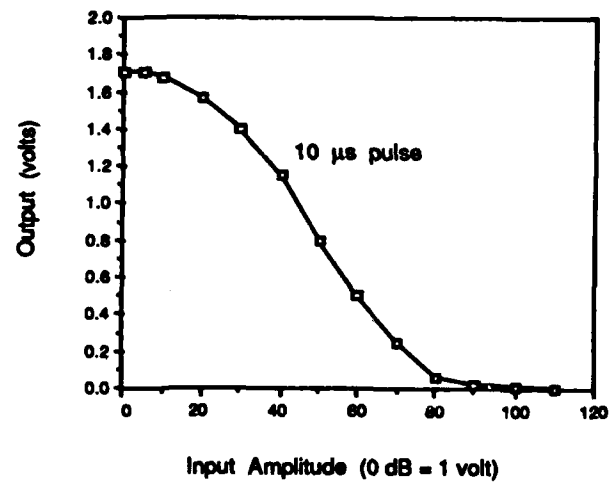
Thus, strictly speaking, the circuit yields the "rectified impulse" of the transient, defined by

$$\int_0^{\infty} |v| dt \quad \text{or} \quad \int_0^{\infty} |i| dt \quad .$$

The integral measurement is of great interest, since it also gives an indication of the duration of a pulse (since the peak amplitude is known). One pitfall intrinsic to the measurement of these pulse integrals should be noted: Since the pulse integral is proportional to both amplitude and duration, each of which is specified over a 60-dB dynamic range (10 V/m to 10 kV/m and 10 ns to 10  $\mu$ s, respectively), this parameter can vary over 120 dB. Since this entire range cannot be measured by a single integral detector of reasonable complexity, two options exist to deal with this:

- We could measure a portion of this range. This portion could be selected through consultation with IMPS experimenters to ensure that each monitored experiment receives the data most useful to it.
- The design could undergo further development to accommodate a greater dynamic range at some expense. We have, in fact, been able to expand the dynamic range of the integral circuit to approximately 80 dB (Figure 22).

**a. Response with Respect to Amplitude**



**b. Response with Respect to Time**

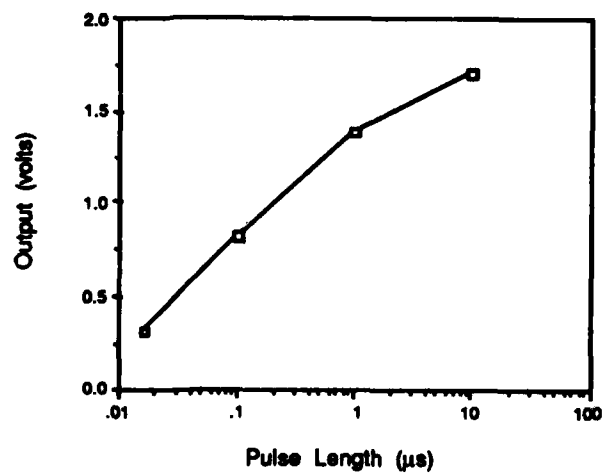


**Figure 22. TPM Integral Detector Response.**

#### **3.3.1.4 Pulse Counter**

The pulse counter function is divided between the pulse analyzer circuitry and the digital interface hardware and software. The pulse analyzer produces a signal proportional to the peak magnitude of the input pulse. The interface compares this value to a preset threshold and counts up to 15 events that exceed the threshold within a telemetry frame. This process is described further in Section 3.3.2.2.

#### **3.3.1.5 Pulse Analyzer Performance Summary**

The pulse analyzer performance characteristics for SRI's TPM system match or exceed our design goals. The TPM system is able to measure pulses whose total duration is between 5 ns and 10  $\mu$ s and whose rise time is between 1 ns and 1  $\mu$ s. Sensitivity of the sensors will be adjusted at integration to provide the proper amplitude response, depending on the sensor configuration. This will be accomplished by employing maximum gain in each channel and inserting in-line attenuation to reduce the signal to appropriate levels.

#### **3.3.2 TPM/TIS Interface**

Since the SCATHA data system accepted analog output from that TPM, new circuitry was required to translate the analog data output from the pulse analyzers into the digital format required for data telemetry and commands on IMPS. The TPM's primary interface is with the SPM experiment built by Aerospace Corporation. The TPM communicates with the IMPS through a joint SPM/TPM interface (called the TIS) built by Aerospace.

##### **3.3.2.1 TPM/TIS Interface Definition**

The TIS design dictated the interface definition (Figure 23). For the sake of simplicity, the interface used is identical to that of the other experiments attached to the TIS.

The TIS puts out a 10 Hz signal (FMB), the rising edge of which signifies its readiness to accept data. The TPM responds by loading

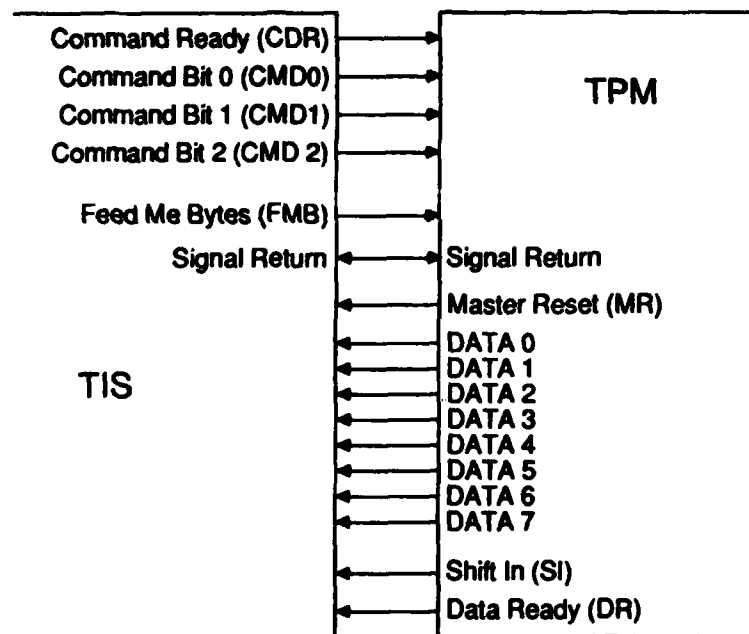


Figure 23. TPM / TIS Interface.

22 bytes of data into a buffer in the TIS. The timing of this transfer is under the control of the TPM, but the TIS requires it to be completed within 25 ms after the FMB signal. Individual bytes are transferred according to the protocol shown in Figure 24. After receipt of the FMB signal, the TPM clears the data buffer in the TIS with the master reset (MR) line. Each byte in turn is then presented on DATA 0-7 and loaded into the buffer by the rising edge of a pulse on the shift in (SI) line. After the last byte has been loaded, the TPM pulses the DR line, signifying that the data are valid and ready for processing by the TIS.

Commands are presented to the TPM on three wires (CMD 0-2), allowing eight different commands. A rising edge on the command data ready (CDR) line signifies that a valid command is being asserted on the CMD 0-2 lines. Commands may arrive at any time.

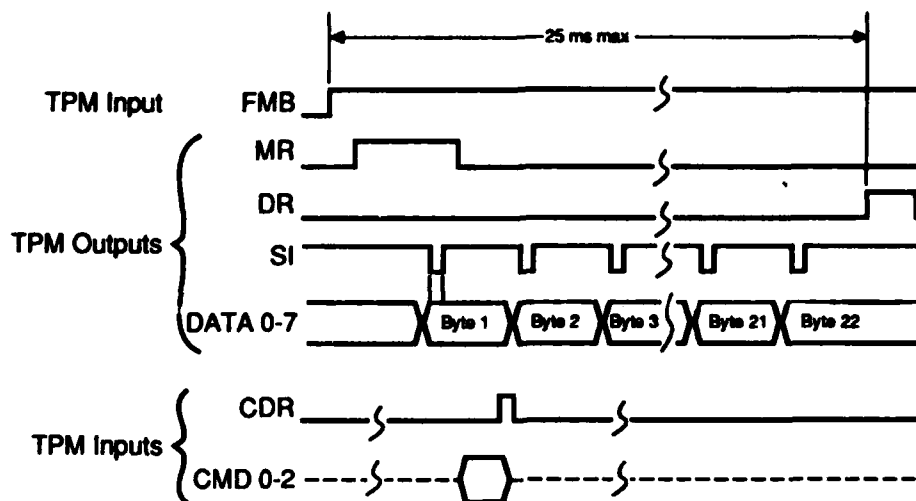


Figure 24. Timing Diagram.

### 3.3.2.2 TPM Interface Circuitry

The interface hardware can be broken down into the following sections:

- Microprocessor and memory
- Multiplexing and A/D
- Pulse comparators/registers
- Command register
- Data output.

Figure 25 shows these elements as they are connected through a central data/address/control bus. Their arrangement corresponds roughly to the detailed circuit diagram in Figure 26.

**Microprocessor and Memory.** An NSC800 microprocessor, running a program stored in a 2 kByte programmable read-only memory (PROM), controls the interface. The NSC800 is a CMOS processor that runs the same instruction set as the Zilog Z-80 NMOS microprocessor. One hundred twenty-eight bytes of random-access memory (RAM) contained in the NSC810 RAM/IO/timer



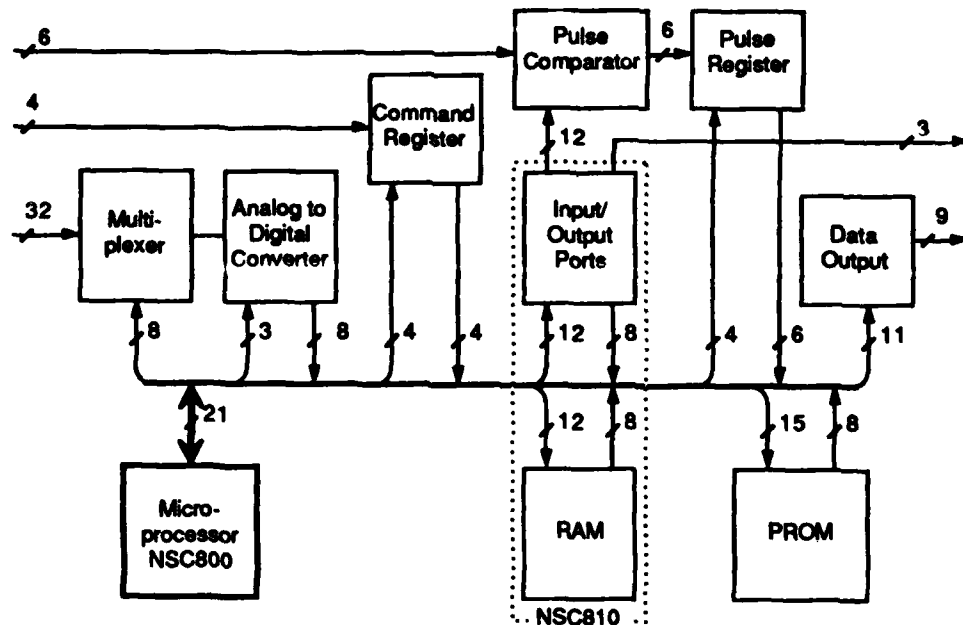


Figure 25. TPM/TIS Interface Block Diagram.

chip are used for a program stack, program variables, and temporary storage of output data.

The NSC800 can address 64K of memory and 256 separate input/output (I/O) locations. The PROM and RAM share the microprocessor's memory space; the other sections of the interface are addressed as I/O. The memory and I/O addresses were assigned so as to minimize the decoding hardware required.

The only input that directly controls the microprocessor is the FMB line, which is connected to its nonmaskable interrupt input. This input cannot be disabled in software and forces the TPM program to run from a particular (fixed) location in memory every time the FMB is asserted.

**Multiplexing and A/D.** A pair of 16-into-1 analog multiplexers selects one of the 32 analog input voltages. The designed output range of the analog circuits is 0 to 4 V; however, since an overload on one of the multiplexer inputs could possibly affect the others, each is protected with series resistors and diode shunts to ground and supply. The selected



voltage is buffered by an op-amp to drive the input of the analog-to-digital converter (A/D). The A/D reference is 4.5 V supplied by an IC voltage regulator. This sets its full-scale input to 4.5 V.

The multiplexers and A/D are configured so that they can be addressed as a single I/O unit by the microprocessor. Executing the NSC800's IN instruction with an address in the range 128 to 159 (decimal) will select the appropriate analog input, convert it, and present the digital representation on the microprocessor's data bus.\* Since the A/D conversion time is longer than the microprocessor's normal I/O read cycle, the A/D's RDY (ready) output is connected to the microprocessor's WAIT input.

**Pulse Comparators/Registers.** The pulse counting function is implemented with a combination of hardware and software.

Six analog comparators continuously monitor the six magnitude outputs from the pulse analyzers. When any of the magnitude outputs exceeds the set detection threshold, it sets high the corresponding bit in the pulse register (which consists of six "D" flip-flops). Each of the bits acts as a flag to signal the detection of one or more pulses since the last time the pulse register was reset. The microprocessor regularly reads the pulse register (reading it also automatically resets it) and counts the pulse events on each channel in memory. The frequency with which the pulse register is checked is governed by software; it is made higher than the maximum pulse repetition frequency (PRF) of the pulse analyzer circuits, so that no valid pulses will go uncounted. However, the occurrence of more than one pulse within a telemetry frame (200 ms) is expected to be rare (based on experience with similar experiments).

The three I/O ports included in the NSC810 are used to set the pulse comparator thresholds and to read the pulse register. The software instruction to read port C (similar in software to reading the analog

---

\*To simplify the hardware while ensuring proper timing of the conversion, an IN instruction actually reads data from the address specified in the previous IN instruction. Since the inputs are always read in the same regular order, this has very little effect on the software.

inputs) also automatically clears the pulse register after loading its contents into port C's input register. This minimizes the chance of a pulse coming in after the register has been read but before it is reset.

Port A and half of port B are used to set the comparator thresholds. Two digital bits are required to set the threshold of each of six channels, thus requiring a total of 12 bit outputs. A resistor network is used to convert each two-bit digital value to an analog voltage at its respective comparator's input.

**Command Latch.** A four-bit latch is used to store commands until the microprocessor can process them. The rising edge of the CDR input stores the value of the three-bit command. It also sets the most significant bit of the command latch high, so that the microprocessor can detect the presence of Command 0. The value stored in the command latch is addressed using the same IN instruction as the other I/O circuitry; it is cleared by writing a dummy byte (whose value is ignored) to the same location.

**Data Output.** The data output signals are MR, shift in (SI), DR, and the eight data lines (DATA 0-7). MR and DR are addressed as bits of Port B on the NSC810, and thus must be explicitly set and reset at the appropriate time by the program. SI is generated directly from the microprocessor's address and write control lines when the data output is addressed with the NSC800's OUT instruction. The rising edge of SI is timed in relation to the latched data outputs so that the data set-up and hold time requirements of the TIS data buffer are met with a large margin.

### **3.3.2.3 Interface Software**

The TPM interface hardware allows independent control of each of the following functions from software:

- Digitize 1 of 32 channels
- Read the command latch
- Reset the command latch
- Read the pulse comparator thresholds
- Set the pulse comparator thresholds

- Read and reset the pulse register
- Send out an individual byte
- Turn on the DR, MR, and/or ARS lines
- Turn off the DR, MR, and/or ARS lines.

The above software-controlled hardware functions and the internal capabilities of the microprocessor are combined to perform the following required TPM system functions:

- Convert 32 analog voltages to digital
- Calculate parity bits for analog data
- Respond to commands
- Maintain pulse counts for six channels
- Pack parity, command, and pulse count data into compact formats
- Send out data and status bytes in accordance with TIS interface protocol.

**Program Structure.** Figure 27 illustrates the flow of the program. It consists of a main program loop and an interrupt service routine. The main program initializes the system when power is first applied, then enters an infinite loop that maintains the pulse counts while waiting for an FMB interrupt. The use of the nonmaskable interrupt to drive the main timing of the program makes it immune to software latchups, since the interrupt always forces it to a fixed, known address in ROM.

The main data-conversion and data-transmission functions of the TPM interface are performed only in response to an FMB interrupt from the TIS. The TPM telemetry frame, during which it digitizes all the pulse analyzer data and sends out 44 bytes of data and status information, is 200 ms. Since that period is twice as long as the TIS's data collection interval, the TPM responds differently to alternate FMB pulses. On the first half-cycle, the TPM digitizes all its analog data and sends out the first 22 bytes of information; on the second, it sends out the remaining 22 bytes.

The program keeps a byte in memory that indicates the current half-cycle. When it receives an FMB, it first checks the value of that byte to determine which portion of the interrupt routine to run. Since this

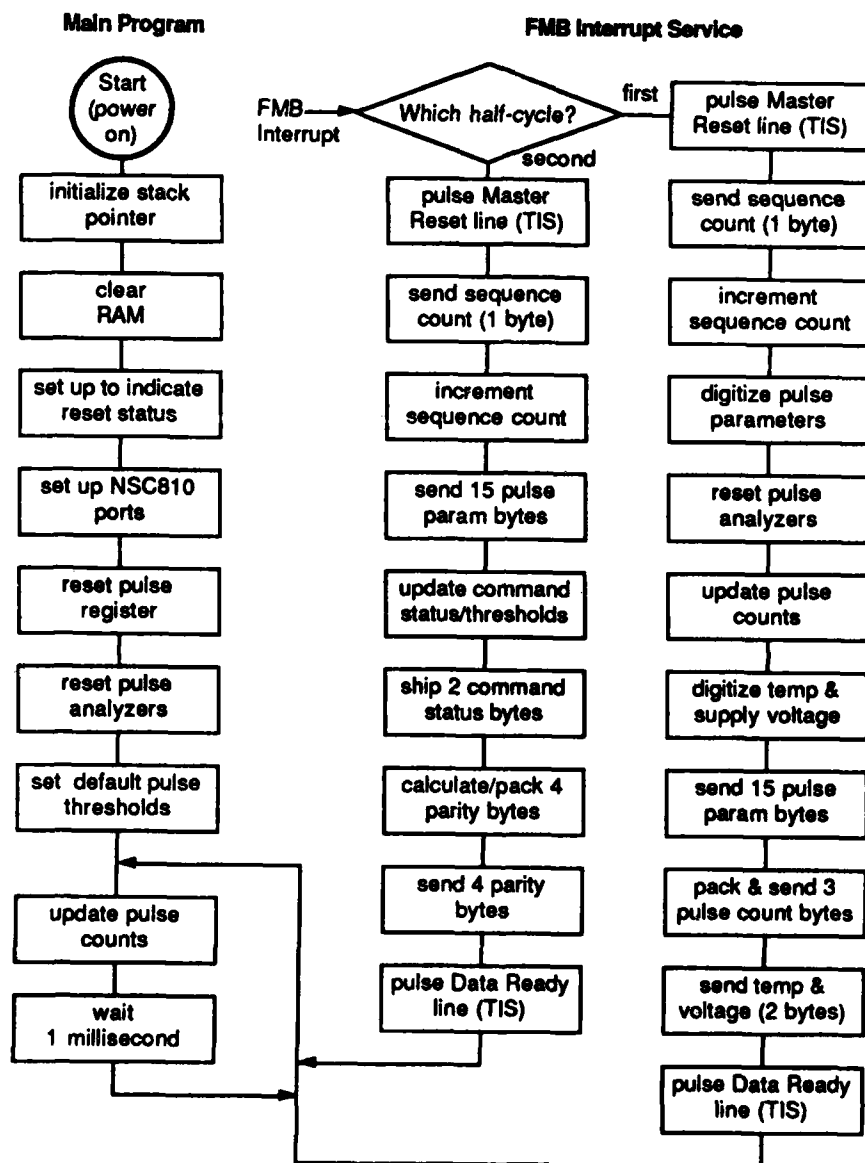


Figure 27. Overall Program Flow.

process is crucial to the proper operation of the program, the program actually counts how many "1" bits the half-cycle byte contains. If it contains four or more ones, the second half-cycle is executed; otherwise it executes the first. Thus, the program can tolerate up to three hard bit errors in the half-cycle byte's memory location without losing sequence. The sequence counts transmitted with each packet are also checked to ensure they correspond to the actual half-cycle executed. If for any reason a half-cycle is skipped, the transmitted sequence counts will reflect that condition.

Initialization. The stack pointer is set initially to the top of RAM and grows down. During normal program operation, the stack should be no more than 6 bytes deep, but it could grow considerably larger without interfering with the other areas of memory. Immediately after initializing the stack pointer, the program pushes the address 0000 onto the stack. This ensures that if the stack underflows for any reason, the program will restart in an orderly manner. The program also sets the sequence number to zero, fills the data memory with the ASCII code for "R," and sets the half-cycle indicator so that the second half-cycle will be executed in response to the next FMB. Thus, the first packet after a reset will be clearly identifiable as such.

Pulse Count Function. For each of the six sensor channels, the Pulse\_count subroutine maintains a count of the number of pulses that have exceeded that channel's threshold during the telemetry frame. When called, it loads the contents of the pulse register into the micro-processor's accumulator register (which automatically clears the pulse register). If the value of the register is zero, it immediately returns to the calling program. If the pulse register was nonzero, Pulse\_count checks each of the six bits; for each "1" bit, it increments the value of the corresponding pulse count in memory. Since pulse counts are expected to exceed 1 only rarely, they are restricted to a maximum value of 15. This allows two pulse counts to be packed into one byte when they are sent to the telemetry system. However, the program does not allow the pulse

count to "roll over" if more than 15 pulses are detected. A pulse count of 15 indicates 15 or more pulses.

Since the pulse analyzer circuitry treats events occurring within a few milliseconds of each other as one event, running Pulse\_count every millisecond is adequate to ensure that all detectable pulses will be counted. The hardware is configured so that a single pulse that overlaps several sampling periods will only be counted once.

**Data Conversion.** The actual digitization of the analog parameter data occurs immediately before the first 15 are sent to the TIS (during the first packet). The hardware and software are configured to make the conversion as quickly as possible. It would have been desirable to sample the data simultaneously, but to do so would have required substantially more weight, size, and power. The TPM digitizes 30 analog pulse parameters in approximately 350  $\mu$ s, less than 0.2% of the telemetry frame. Immediately after digitizing the data, the program resets the analog detectors.

**Data Transmission and Packet Structure.** During each telemetry frame the TPM sends 44 bytes to the TIS, allocated as shown in Figure 28. The data transmitted are of four types: pulse parameter data, pulse counts, circuit housekeeping, and program status.

The first byte of each data packet is a sequence count. The sequence count is incremented on each half-cycle, so that it rolls over every 128 telemetry frames. It is intended to be used as an indicator of proper program execution and a quick means of identifying which information the packet contains, rather than as a primary timing reference. An odd sequence number indicates the first half-cycle; an even or zero sequence number indicates the second.

The pulse parameter data include five parameters from each of the six channels: peak positive amplitude, peak negative amplitude, peak positive rate of rise, peak negative rate of rise, and pulse integral. Each of these takes one byte, for a total of 30 bytes. These data are evenly divided between the two packets. If one packet is lost, complete pulse



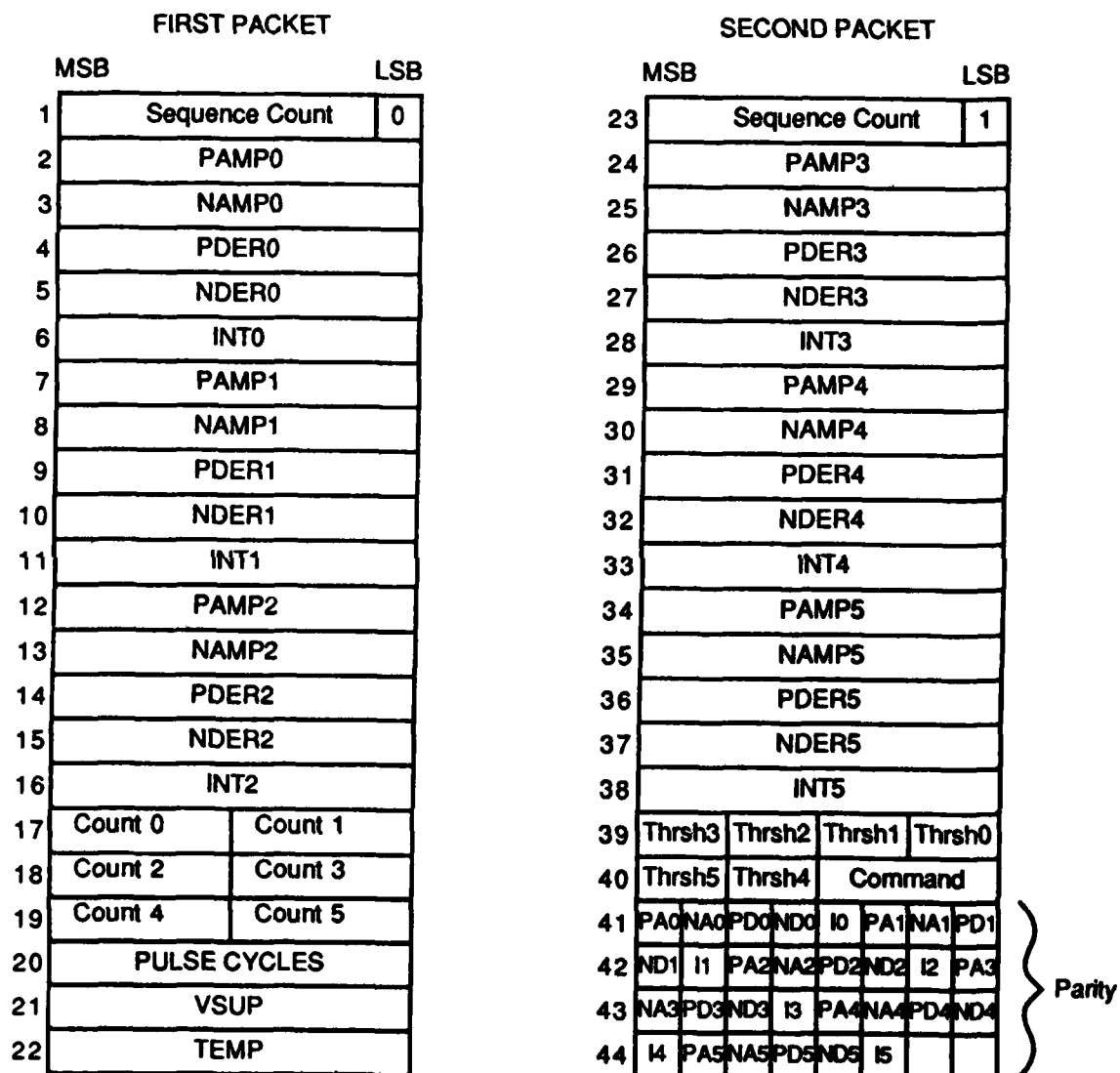


Figure 28. TPM Packet Structure.

parameter data will still be available for three of the channels. A parity bit is calculated for each of the 30 pulse parameter data. These are packed into four bytes and sent at the end of the second packet.

The six pulse counts are packed into three bytes (since they are restricted to four-bit values) and sent as a group in the first packet.

The remaining bytes are used to report the status of the instrument. Two bytes in the first packet contain measurements of the temperature and supply voltage of the TPM. The "pulse cycles" byte tells how many times the Pulse\_count routine was run during the last telemetry frame. During normal operation this number should be constant within two counts. Finally, two bytes are devoted to the status of the pulse comparators and command interface. Two bits are used for the current value of the threshold for each of the six channels (these are actual values read from the threshold latches, not from memory). The remaining four bits report the last value read from the command latch. Zero indicates no command was received; if the most significant bit is set, it indicates that the lower three bits contain a command.

### **3.3.3 Power Supply**

The central processor includes circuitry to convert the satellite's 24 to 32 V supply to the voltages required by the TPM circuitry (Figure 29). As in previous SRI satellite instruments, it is based on a switching power supply designed to minimize heat dissipation. Special care was devoted to tailoring the switched waveform and the use of line filtering to prevent radiated or conducted interference with other circuitry. The regulator design provides the required immunity to voltage fluctuations and high-frequency interference spikes that may be found on the prime power supply lines, especially those expected when IMPS is connected to shuttle power. It includes circuitry to limit in-rush current when power is first applied and automatically shuts down in the input voltage falls below approximately 20 V. The power supply's current profile after turn-on is shown in Figure 30.

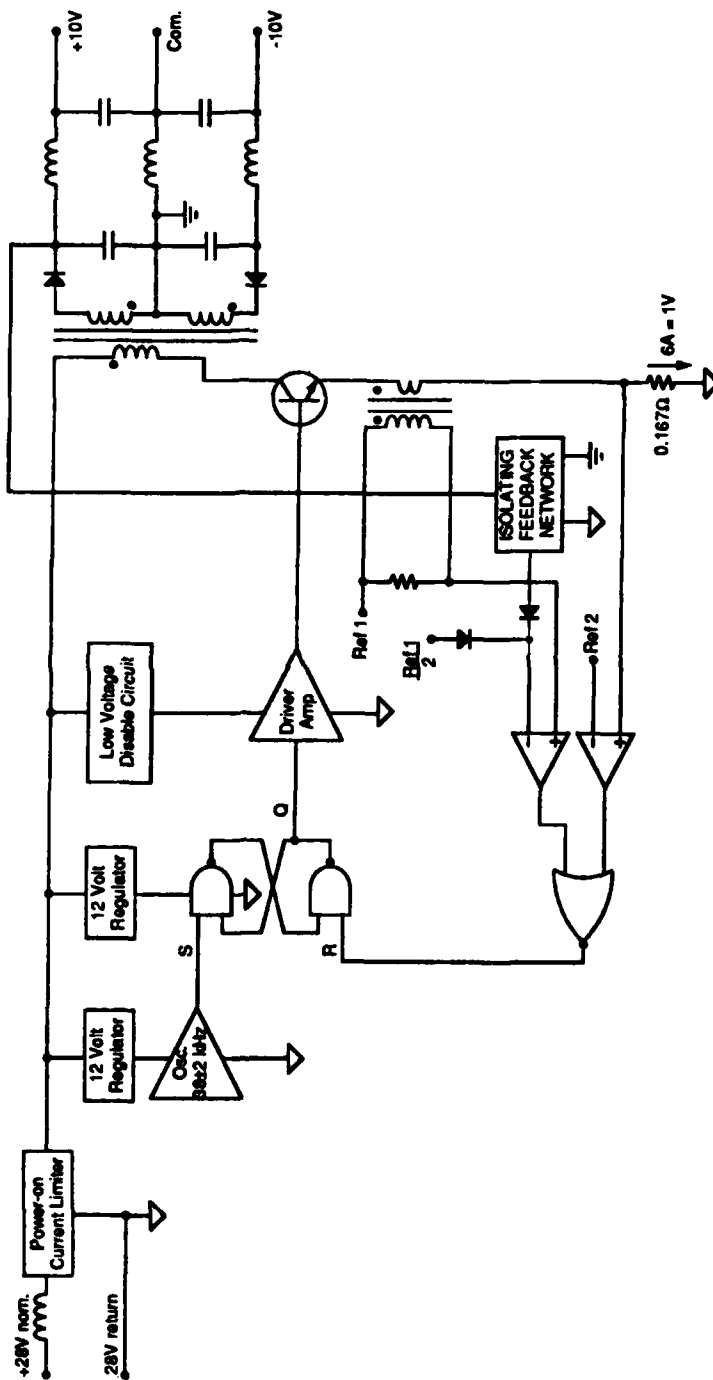


Figure 29. Power Supply Schematic.

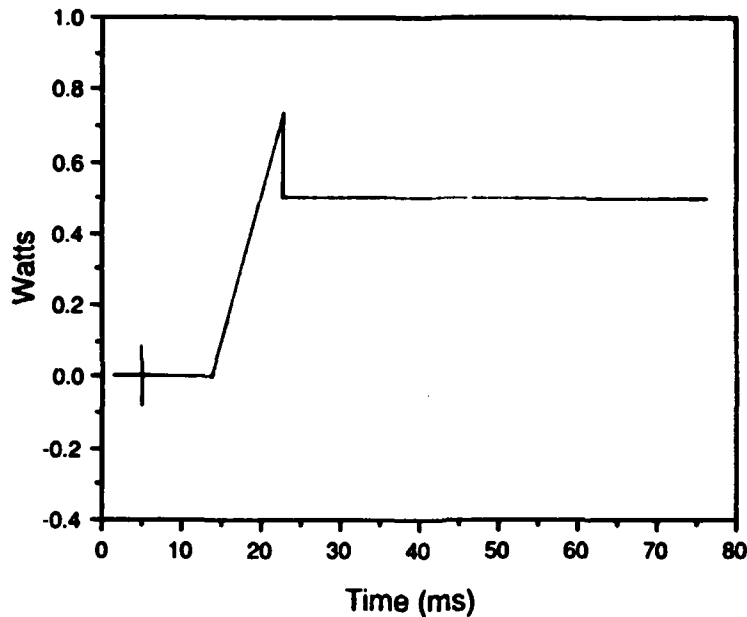


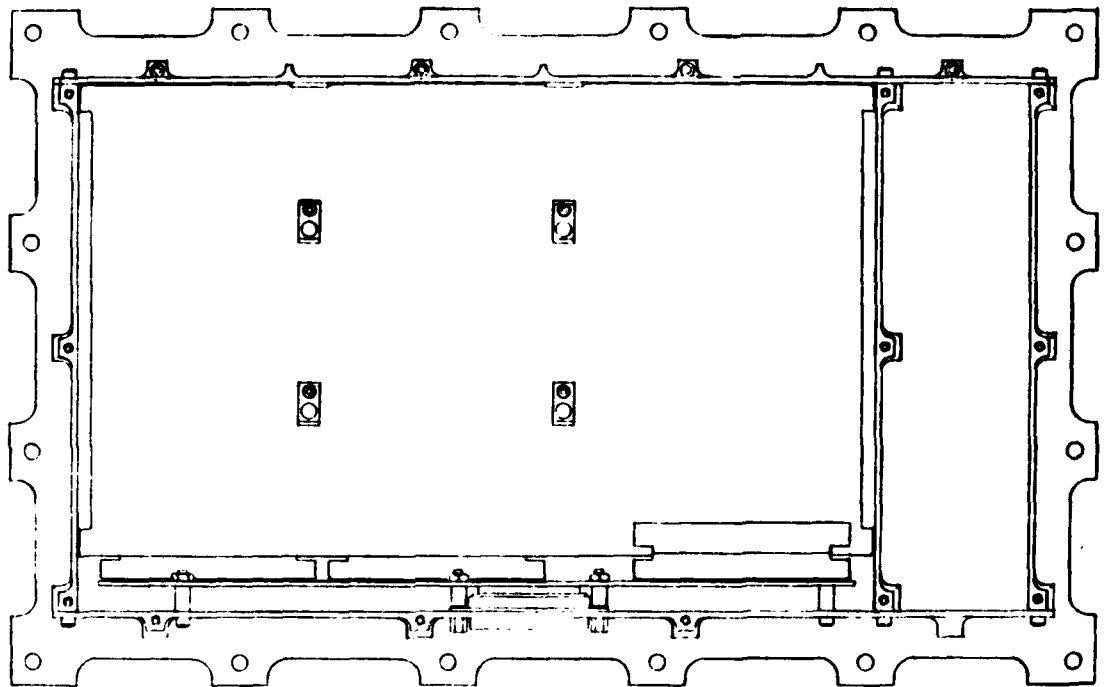
Figure 30. Power Profile.

#### 3.3.4 Mechanical Design

The central processor is housed in an aluminum box (Figure 31). A stack of several circuit boards, containing the six pulse analyzer channels and the digital interface, occupies most of the space. The boards have edge connectors that mate with a vertical motherboard on one side of the box. The other three sides of the boards are supported by aluminum ribs and retained there by spring clips, ensuring good mechanical and thermal contact around the periphery. The boards are also supported in the middle at four points arranged to suppress mechanical resonances and also provide thermal conductivity.

The power supply occupies a separate compartment at one end of the box. The power supply and the digital interface are both electromagnetically partitioned from the analog boards to prevent interference with the sensitive analog detector circuits.

a. Top View



b. Side View

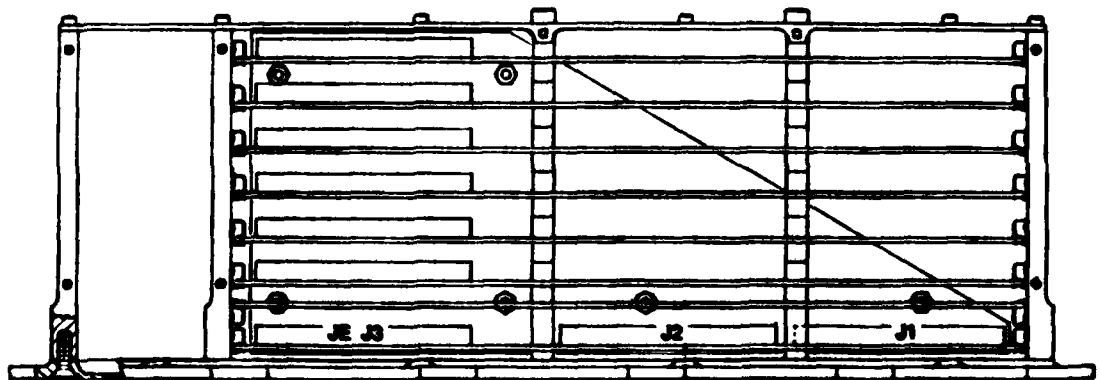


Figure 31. Box Design.

### 3.4 Ground-Support Equipment

The TPM GSE, used to test the TPM on the ground, consists of a program running on an Apple Macintosh computer, hardware designed to simulate the TIS interface, and a calibration stimulus. Figure 32 illustrates the GSE system. The IMPS power interface simulator is to be furnished by the project.

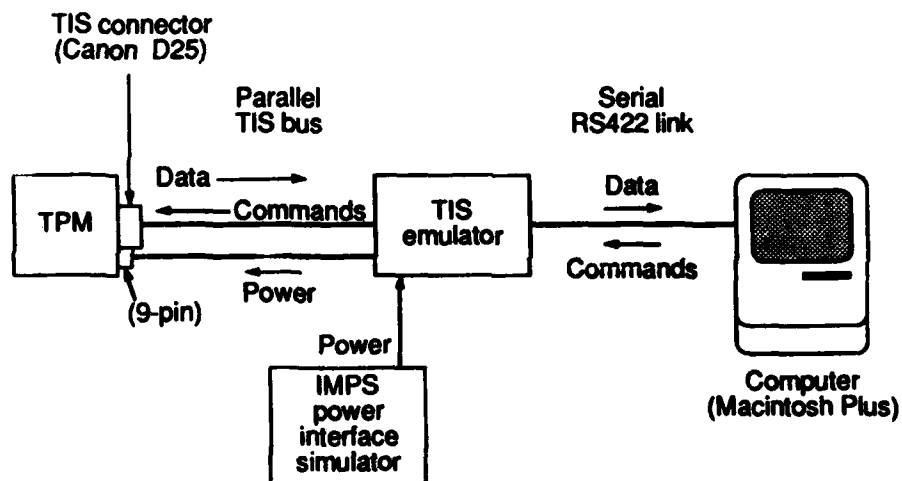


Figure 32. GSE Hardware and Control / Monitor Functions.

#### **3.4.1 TIS Emulator Hardware**

The GSE hardware connects on one side to the Macintosh's RS-422 serial port; on the other it produces FMB and command signals and receives data from the TPM. To provide the most accurate simulation, the data buffer for the TPM interface consists of the same first-in, first-out (FIFO) memory chips used in the TIS.

#### **3.4.2 Software**

The GSE software allows the real-time display of all TPM data in text mode (Figure 33), or of a single channel's data in simulated strip-chart form (Figure 34). FMBs can be sent manually or automatically at several rates, including the 10 Hz operating rate of the TIS. Commands can also be sent under manual control. All data are accumulated in memory while the program is operating, and data from any or all channels can be saved on a hard disk or floppy disk. The user can set an "event threshold" below which data will be ignored. This allows small nonzero data resulting from noise to be excluded. A packet of data will be recorded if it contains any value larger than the event threshold. The program also checks parity for those data whose parity is transmitted, and senses errors in sequence number, packet length, and transmission time.

#### **3.4.3 Calibration Stimulus**

The calibration stimulus (Figure 35) is an electronic device that produces the waveform shown in Figure 36. The duration of the successive voltage levels is much longer than the TPM pulse analyzers' time constant, so that the TPM measures the characteristics of only the fast transitions between levels. These transitions can be controlled and precisely measured in the laboratory. The stimulus is battery-powered so that it can be used in situ without disturbing the grounding on the carrier after integration.

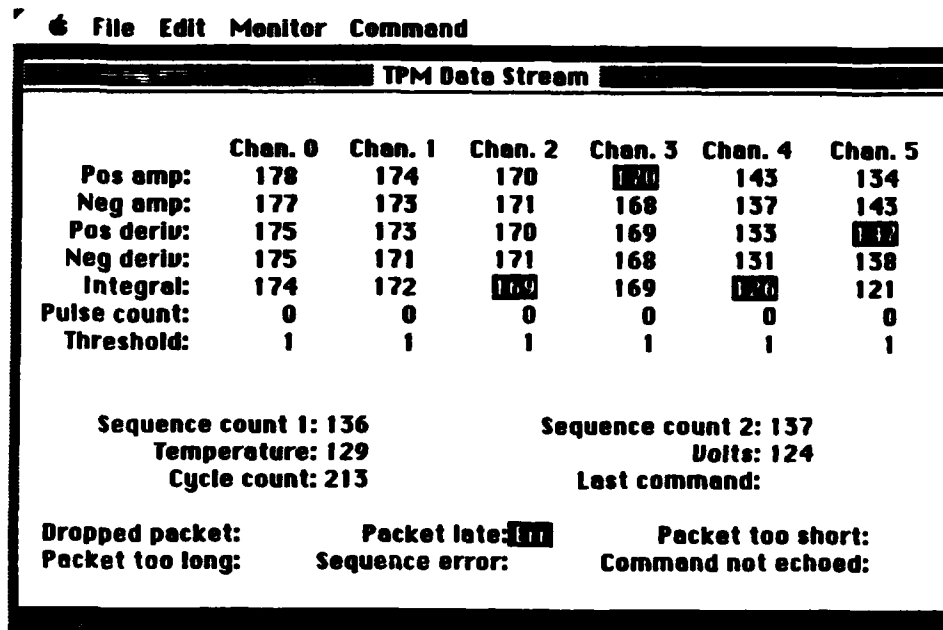


Figure 33. Control Monitor GSE: Text Display.

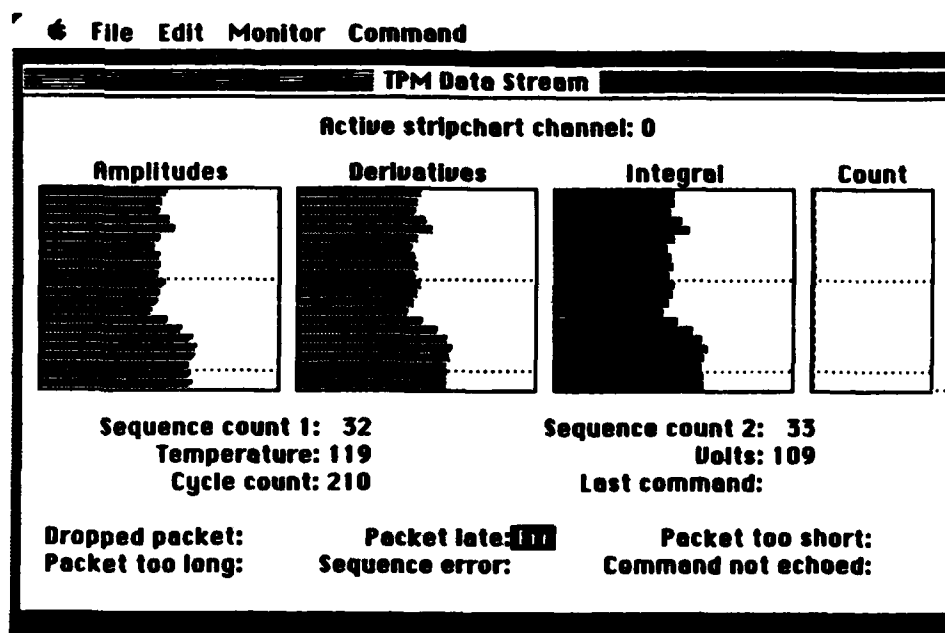
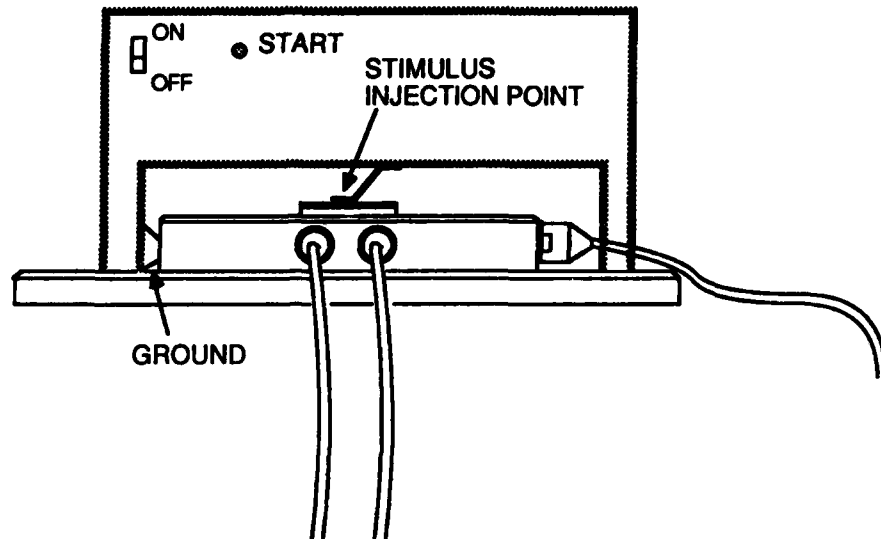
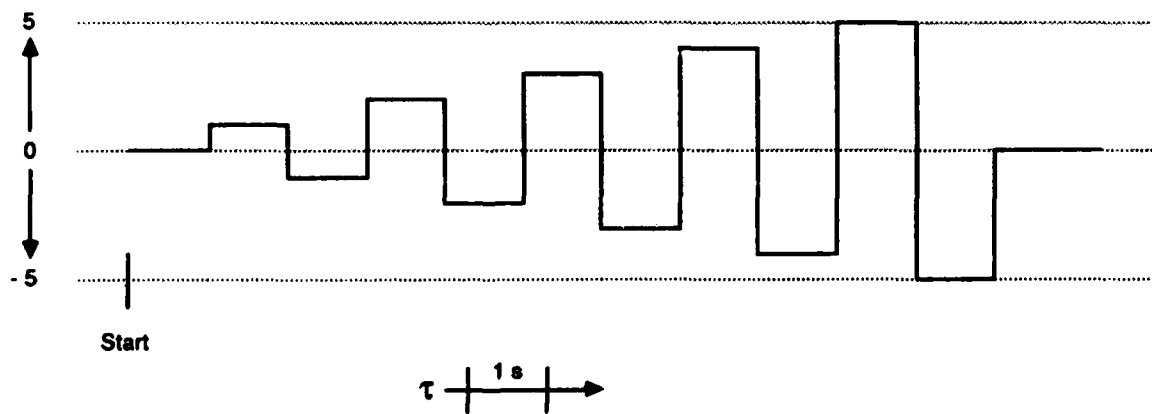


Figure 34. Control Monitor GSE: Stripchart Display.





**Figure 35. GSE Hardware, Sensor Stimulus Configuration.**



**Figure 36. Sensor Stimulus Sample Waveform.**

#### 4.0 PERFORMANCE SUMMARY

TPM performance is summarized in Tables 2, 3, and 4. In Table 2, all measured values are the maximum detected during the telemetry frame (optimized for 200 ms). Voltages are at the pulse analyzer input; sensitivity with respect to electric field will be adjusted according to system noise level during integration.

**Table 2**  
**MEASUREMENT RANGES**

Parameter	Value
Peak amplitude	1 mV to 1 V (50 ns pulse)
Peak rate of rise	10 V/ $\mu$ s to 3000 V/ $\mu$ s (100 ns to 300 ps rise time)
Integral	1 nVs to 3 $\mu$ Vs, as follows: 0.1 mV to 0.3 V magnitude for 10 $\mu$ s pulse; 10 ns to 10 $\mu$ s length for 0.3 V magnitude
Pulse counts	0 to 15 pulses
Count thresholds	22%, 44%, 67%, 89% of full scale

**Table 3**

**CARRIER RESOURCES**

Carrier	Volume (cm <sup>3</sup> )	Mass (kg)	Power (W)
Digital circuitry	1000.0	0.29	0.58
Analog circuitry (each of 6)	1000.0	0.34	1.29
Power supply	1620.0	0.7	*
Enclosure	8900.0	(2.0)	-
<b>Total with enclosure</b>	<b>8900.0</b>	<b>(5.0)†</b>	<b>(13.0)</b>
Current sensor	5.2	0.08	0
E-field sensor (each of 5)	117.0	(0.15)	(0.1)
<b>Sensors total</b>	<b>590.0</b>	<b>(0.83)</b>	<b>(0.5)</b>
<b>TOTAL</b>	<b>9490</b>	<b>(5.8)</b>	<b>(13.5)</b>

\* 70% estimated efficiency.

† Parenthetical values are estimated; others are measurements of prototype units.

**Table 4**

**TEMPERATURE REQUIREMENTS (C°)**

Condition	Required Temperature
Flight preferred	+20
Flight operating range	0 to +50
Flight nonoperating range	-30 to +60
Survival range	-30 to +75
Ground operating range	0 to +50
Ground nonoperating range	-30 to +60

## REFERENCES

- Adamo and Nanevicz
- 1983 R. C. Adamo and J. E. Nanevicz, "Development of a Continuous Broad-Energy-Spectrum Electron Source," Proceedings of the Spacecraft Environment Interactions Conference, NASA/Lewis Research Center, October 1983.
- 1979 R. C. Adamo and J. E. Nanevicz, "Chemical Physics of Charge Mechanisms in Nonmetallic Spacecraft Materials," Final Report, Contract F49620-77-C-0113, SRI Project 6402, SRI International, Menlo Park, California, May 1979.
- 1977 R. C. Adamo and J. E. Nanevicz, "Effects of Illumination on the Conductivity Properties of Spacecraft Insulation Materials," Final Report, SRI Project 4904, NASA CR-135201, Contract NAS3-20081, SRI International, Menlo Park, California, July 1977.
- 1976 R. C. Adamo and J. E. Nanevicz, "Spacecraft-Charging Studies of Voltage Breakdown Processes on Spacecraft Thermal Control Mirrors," Progress in Astronautics and Aeronautics, Vol. 47, American Institute of Aeronautics and Astronautics, New York, New York, 1976.
- DeForest
- 1972 S. E. DeForest, "Spacecraft Charging at Synchronous Orbit," J. Geophys. Res., Vol. 77, No. 4, February 1972.
- Gussenhoven et al.
- 1985 Gussenhoven et al., "High-Level Spacecraft Charging in the Low-Altitude Polar Auroral Environment," J. Geophys. Res., Vol. 90, No. A11, November 1985.
- Katz et al.
- 1977 I. Katz et al., "Dynamic Modeling of Spacecraft in a Collisionless Plasma," Proceedings of the Spacecraft Charging Technology Conference, AFGL-TR-77-0051, Air Force Geophysics Laboratory, February 1977, ADA045459.
- Mizera et al.
- 1981 P. F. Mizera et al., "First Results of Material Charging in the Space Environment," Aerospace Report TOR-0081(6506-01)-1, Contract F04701-80-C-0081, Space Division Air Force Systems Command, Los Angeles Air Force Station, March 1981.

Nanevicz and Adamo

- 1984 J. E. Nanevicz and R. Adamo, "Laboratory Studies of Spacecraft Response to Transient Discharge Pulses," Proceedings of the Spacecraft Environmental Interactions Conference, NASA/Lewis Research Center, October 1984.
- 1977 J. E. Nanevicz and R. C. Adamo, "A Rugged Electron/Ion Source for Spacecraft Charging Experiments," Proceedings of the Spacecraft Charging Technology Conference, AFGL-TR-77-0051, pp. 549-555, Air Force Geophysics Laboratory, Hanscom AFM, 24 February 1977, ADA045459.

Nanevicz et al.

- 1980 J. E. Nanevicz et al., "Electromagnetic Fields Produced by Simulated Spacecraft Discharges" AFGL-TR-81-0270, 1980 Spacecraft Charging Technology, NASA Conference Publication 2182, November 1980, ADA114426.
- 1975 J. E. Nanevicz et al., "Electrical Discharges Caused by Satellite Charging at Synchronous Orbit Altitudes," 1975 Lightning & Static Electricity Conference, Culham Laboratory, Oxford, England, 1975.

Purvis et al.

- 1977 C. K. Purvis, N. J. Stevens, and J. C. Oglebay, "Charging Characteristics of Materials: Comparison of Experimental Results with Simple Analytical Models," Proceedings of the Spacecraft Charging Technology Conference, AFGL-TR-77-0051, Air Force Geophysics Laboratory, NASA TMX-73537, February 1977, ADA045459.

Stevens and Vampola

- 1978 J. R. Stevens and A. L. Vampola, "Description of the Space Test Program P78-2 Spacecraft and Payloads," Final Report SAMSO TR-78-24, Space and Missile Systems Organization Air Force Systems Command, October 1978.

Stevens et al.

- 1977 N. J. Stevens et al., "Testing of Typical Spacecraft Materials in a Simulated Substorm Environment," Proceedings of the Spacecraft Charging Technology Conference, AFGL-TR-77-0051, Air Force Geophysics Laboratory, February 1977, ADA045459.

Vampola

- 1980 A. L. Vampola, "P78-2 Engineering Overview," AFGL-TR-81-0270, 1980 Spacecraft Charging Technology, NASA Conference Publication 2182, Air Force Geophysics Laboratory, November 1980, ADA114426.

Vance

- 1980 E. F. Vance, "Electromagnetic-Interference Control," IEEE Trans. EMC, Vol. EMC-22, No. 4, pp. 319-328, November 1980.